DOI: 10.15587/978-617-8360-09-2.CH4

Bogdana Gayvas, Yevhen Chaplya, Veronika Dmytruk,
Bogdan Markovych, Anatolii Dmytruk

CHAPTER 4

DRYING OF A POROUS LAYER IN AN EXTERNAL CONSTANT ELECTRIC FIELD (ELECTROOSMOTIC DRYING)

ABSTRACT

In this Chapter, mathematical modeling of the drying process of a porous layer under the influence of an external constant electric field is presented, taking into account the electroosmotic effects on mass and heat transfer. A mathematical model of electroosmotic drying is formulated based on the coupled equations of moisture transport, electrokinetic flow, and thermal effects. The analysis considers both natural and convective drying conditions, incorporating the impact of electroosmotic forces on moisture migration within the porous medium.

In the study, the fundamental mechanisms governing electroosmotic moisture removal are explored, including the formation of a double electric layer at the interface between the pore liquid and the solid skeleton, the competition between electroosmotic and capillary forces, and the transition between different drying regimes. A system of governing equations, including modified Stefan-Maxwell relations and generalized Darcy's law, is derived to describe the transport processes in the porous domain.

Numerical simulations are carried out. The experiments have demonstrated the effect of key parameters, such as electric field intensity, moisture content, temperature, and mass transfer coefficients, on drying kinetics. Results indicate that increasing the electric field intensity significantly accelerates moisture removal, particularly during the initial drying stage when electroosmotic forces dominate.

KEYWORDS

Electroosmotic drying, porous media, moisture transport, external electric field, capillary effects, ponderomotive force, convective drying, unilateral drying, bilateral drying, boundary layer properties, isothermal drying, electrokinetic flow, sustainable technology, numerical methods.

In drying processes, external mass transfer can be intensified through an active hydrodynamic regime in the near-wall layer, induced by the action of external physical fields of various natures [1–10]. Thus, the application of physical fields can stimulate efficient moisture removal from wet materials.

The works [11–14] explore the feasibility of using electroosmosis for moisture removal from various dispersed systems. These studies emphasize the role of electrokinetic properties in the process of liquid transport and separation under an applied electric field. The study by O. Berezniak [15] presents an experimental investigation of electroosmotic dewatering of kaolin, highlighting the potential practical application of this drying method.

The possibility of using electroosmosis for mass transfer intensification is associated with the existence of a double electric layer at the interface between the pore liquid and the solid skeleton. This concept has been explored in theoretical and experimental studies [16–18], demonstrating how electrokinetic effects influence moisture movement in porous media and complex dispersed systems. To the issues of intensification of heat and mass transfer processes under the influence of an external electric field are devoted the works [19–21]. They have demonstrated the role of electromagnetic fields in controlling thermal stresses and optimizing heating modes in electrically conductive materials.

In [16], L. Lysenko has analyzed electrokinetic soil purification, which shares fundamental principles with electroosmotic drying.

Mathematical modeling has played an important role in understanding electroosmotic drying processes. The works [22, 23] have focused on the mathematical representation of moisture transport in porous bodies, considering phase transition kinetics and deformations.

Additionally, research on applied electroosmosis has extended to diverse fields, including industrial drying and food processing. Studies such as those by O. Severyn and A. Fariseev [24, 25] investigated drying systems enhanced by electroosmotic effects, demonstrating their potential in improving energy efficiency and process control.

Moreover, electroosmosis has been studied for its influence on multiphase systems and reactive environments [26, 27]. The interplay between electrokinetic forces and fluid dynamics in these systems suggests promising applications for controlling moisture distribution and enhancing separation processes.

The possibility of using electroosmosis for moisture removal from a body is associated with the existence of a double electric layer at the interface between the pore liquid and the solid skeleton. The presence of electric forces alters the nature of the drying process.

At the initial stage, a dried zone forms within the body only near a portion (S_1) of the surface (S) on the side of the acting forces (dried Zone 1). The other part (S_2) of the body's surface remains moist, and if the electric force exceeds the capillary force caused by the curvature of the liquid-gas contact surface, electroosmotic liquid outflow will occur through this region. The liquid-gas phase transition surface is denoted by S^*.

As the dried zone expands, its electrical resistance and voltage drop increase. Consequently, the voltage and the electric field intensity in the liquid-filled region will decrease. The reduction in liquid content during drying will also lead to a decrease in its total electric charge. The ponderomotive force $\rho_q\vec{E}$ (ρ_q is the average charge density of the diffuse layer, $\vec{E}$ is the electric field intensity in the pores) acting on the liquid due to the electric field will diminish throughout the drying process. Meanwhile, the capillary force remains nearly unchanged at this stage.

Once these forces reach equilibrium, the electroosmotic liquid outflow through the surface (S_2) ceases, and a dried zone also begins to form there. From this moment, the dried zones propagate inward from the surfaces (S_1) and (S_2), moving toward each other. Thus, the drying process occurs in two stages:

The 1st stage of drying.

The mass transfer equations in the dried zone and the boundary conditions will be assumed under the following formulation:

$$\vec{\nabla}\cdot\left[\rho_v \frac{K_g}{\mu_g}\vec{\nabla}\left(\frac{\rho_a}{M_a}+\frac{\rho_v}{M_v}\right)RT + D'\vec{\nabla}\rho_v\right]=0, \tag{4.1}$$

where ρ_v is water vapor density; ρ_a is air density; K_g is permeability coefficient of the porous medium, depending on the radius and shape of the pores; μ_g is dynamic viscosity coefficient of the gas; M_a is molar mass of air; M_v is molar mass of water vapor; R is universal gas constant; T is temperature; $D`$ is effective binary diffusion coefficient in the pores.

On the moving surface (S^*), the vapor density can be assumed to be equal to the saturated vapor density [28, 29]:

$$\rho_v = \rho_{vn}. \tag{4.2}$$

The form of the boundary conditions on the surface (S) depends on the method of modeling the interaction between the body and the surrounding environment.

In the case under consideration, where the body is in contact with an environment consisting of an air-vapor mixture on the surface (S) under natural drying conditions, it can be assumed that at a sufficient distance from the surface (S), the vapor density ρ_{ve} and air density ρ_{ae} reach constant values ρ_{v1} and ρ_{a1}, respectively, which are characteristic of atmospheric air, i.e. [3, 12, 35, 36]:

$$\lim_{r\to\infty}\rho_{ve} = \rho_{v1}, \ \lim_{r\to\infty}\rho_{ae} = \rho_{a1}, \tag{4.3}$$

where r is the distance from the surface (S).

In the region external to the body, mass transfer processes will be described by the Stefan-Maxwell equations under the assumption of constant atmospheric pressure:

$$\vec{\nabla}\rho_{ae} - \frac{\rho_{ae}}{D'_e}\vec{V}_e = 0,$$

$$\vec{\nabla}\cdot\left(\vec{\nabla}\rho_{ve}-\frac{\rho_{ve}}{D'_e}\vec{\upsilon}_e\right)=0, \tag{4.4}$$

$$P_{ge}=\left(\frac{\rho_{ae}}{M_a}+\frac{\rho_{ve}}{M_v}\right)RT=const. \tag{4.5}$$

On the surface (S), the normal component of the vapor flux from the drying body must be continuous, i.e.:

$$\vec{n}\cdot j_v=\left(\vec{\nabla}\rho_{ve}-\frac{\rho_{ve}}{D'_e}\vec{v}_e\right)\cdot\vec{n}, \tag{4.6}$$

as well as the component densities of the mixture, which follow from the equality of partial pressures at the surface (S):

$$\rho_{ae}=\rho_a,\ \rho_{ve}=\rho_v. \tag{4.7}$$

Equations (4.1)–(4.7) form a complete system of relations and can be used to describe mass transfer under natural drying of a porous body [30, 31].

At the first stage, the liquid moves under the influence of electric forces toward the surface (S_2) with velocity (Generalized Darcy's law):

$$\vec{\upsilon}_L=\frac{K_L}{\mu_L}\left(\rho_q\vec{E}-\vec{\nabla}P_k\right),$$

where K_L is the permeability coefficient of the body relative to the liquid; μ_L is its dynamic viscosity; P_k is the pressure induced by the curvature of the liquid-gas contact surface. It is possible to assume that the liquid freely exits the pores. At this stage, the phase transition of liquid to vapor near the surface (S_2) will not be considered.

Thus, the amount of liquid in the body will decrease both due to drying from the surface (S_1) and due to electroosmotic removal of moisture through the surface (S_2). The mass balance equation in this case takes the form:

$$\frac{dm}{dt}=-\int\limits_{(S_1)}\left(j_{v1}\cdot\vec{n}_1\right)dS_1-\int\limits_{(S_2)}\left(j_{v2}\cdot\vec{n}_2\right)dS_2, \tag{4.8}$$

where $\vec{n}_1$, $\vec{n}_2$ are the outward normals to the surfaces (S_1) and (S_2), respectively; $\vec{j}_{v1}$ is the vapor flux through the surface (S_1); $\vec{j}_L$ is the liquid flux through the surface (S_2):

$$j_L = \Pi \gamma_L \vec{v}_L. \tag{4.9}$$

The 2^d stage of drying.

At the moment when the electrical and capillary forces balance each other, i.e.:

$$\int\limits_{(V_f)} \rho_q \vec{E} dV_L - P_k S_1^* = 0, \tag{4.10}$$

the liquid outflow ceases, and a second dried zone (Zone 2) emerges, which will expand from surface (S_2) into the depth of the material. In (4.10) (V_L) represents the region of the body occupied by the liquid; V_L is its volume, and S_1^* is the area of the gas-liquid contact surface.

The problem of drying Zone 2 is formulated similarly to the drying problem for Zone 1. The mass balance equation for the moisture in the material now takes the form:

$$\frac{dm_L}{dt} = -\int\limits_{(S_1)} \left(j_{v1} \cdot \vec{n}_1\right) dS_1 - \int\limits_{(S_2)} \left(j_{v2} \cdot \vec{n}_2\right) dS_2. \tag{4.11}$$

Determination of electrical quantities.

The electric field intensity is determined from the corresponding electrostatics problems. For the first stage, the governing equation is given as:

$$\Delta \phi_j = 0,\ \vec{E}_j = -\vec{\nabla} \phi_j,\ \left(j = 1{,}2\right), \tag{4.12}$$

which applies to the region (V_1) (j = 1), bounded by surfaces (S_1) and $\left(S_1^*\right)$, and the region (V_L) (j = 2), occupied by liquid, with the boundary conditions:

$$\phi_1 = \phi_{01} \text{ on the surface } (S_1),\ \phi_2 = \phi_{02} \text{ on the surface } (S_2), \tag{4.13}$$

and the conjugation conditions at the interface:

$$\phi_1 = \phi_2,\ \vec{n}_1 \cdot \left(\vec{j}_1 - \vec{j}_2\right)_1 = 0, \text{ on the surface } (S_1^*), \tag{4.14}$$

where

$$\vec{j}_j = \sigma_j \vec{E}_j,\ \left(j = 1{,}2\right). \tag{4.15}$$

Here, $\vec{j}_1, \vec{j}_2$ are the current density vectors, while σ_1, σ_2 denote the electrical conductivity coefficients in regions (V_1) and (V_L), respectively. The vector $\vec{n}_1$ represents the normal to the interface $\left(S_1^*\right)$.

For the second stage of drying, the electrostatics problem is formulated as:

$$\Delta\phi_m = 0,\ \vec{E}_m = -\vec{\nabla}\phi_m,\ (m = 1,2,3), \tag{4.16}$$

for the regions (V_1) $(m = 1)$, (V_f) $(m = 2)$, and (V_2) $(m = 3)$, bounded by surfaces (S_2^*) and (S_2), under the boundary conditions:

$$\phi_1 = \phi_{01} \text{ on the surface } (S_1),\ \phi_3 = \phi_{02} \text{ on the surface } (S_2), \tag{4.17}$$

and the conjugation conditions:

$$\phi_1 = \phi_2,\ \vec{n}_1 \cdot (\vec{j}_1 - \vec{j}_2) = 0, \text{ on the surface } (S_1^*),$$

$$\phi_2 = \phi_3,\ \vec{n}_2 \cdot (\vec{j}_2 - \vec{j}_3) = 0, \text{ on the surface } (S_2^*), \tag{4.18}$$

where $\vec{n}_2$ is the normal to the surface (S_2^*).

The average charge density of the diffuse layer for a binary electrolyte solution, based on the theory of the double electric layer and works [1, 32, 33], is determined by the formula:

$$\rho_q = \sqrt{\frac{2\varepsilon_f C\Pi}{fRTk_p}\,\frac{zF_f\phi_1}{T_\Gamma}}, \tag{4.19}$$

where ε_f is the average absolute dielectric permittivity of the liquid phase; T_Γ is the tortuosity factor; k_p is the permeability coefficient of the porous medium; ϕ_1 is the surface potential at the closest approach of ions [7]; $z = z_+ = -z_-$, where z_+ and z_- are the valencies of cations and anions; F_f is the Faraday constant; C is the electrolyte concentration; Π is the porosity of the material.

Thus, the problem of electroosmotic drying of a porous body includes the relationships given by (4.1)–(4.9).

It should also be noted that the use of *an isothermal model* for describing electroosmotic drying requires imposing appropriate restrictions on the magnitude of the external electric field.

4.1 ELECTROOSMOSIS DRYING A POROUS LAYER

Let's consider the problem of the influence of electroosmosis influence on drying a porous layer, where free evaporation occurs on one of its surfaces into the external environment, while the other surface is supplied with moisture from a well-permeable wet medium. This problem can model the drying of basements after floods.

A porous layer initially saturated with moisture is examined, with one of its surfaces (Surface 1) in contact with an environment that is a mixture of air and vapor, while Surface 2 borders a well-permeable wet medium.

The air and layer temperatures are assumed to be equal.

Since the vapor in the pores is saturated at the liquid surface, while the surrounding environment is unsaturated, vapor outflow occurs from Surface 1. As a result, a region of dried pores filled with a mixture of air and vapor is formed within the body, where these components are considered separate constituents of the filling gas. During the drying process, this zone expands deeper into the material. The coordinate of the moving boundary is denoted as $z = L_m$.

To intensify the drying process via electroosmotic moisture removal from the porous layer, a constant potential difference is applied between Surfaces 1 and 2. Due to the influence of the electric field on the charge of the diffuse part of the electrical double layer at the solid skeleton-pore liquid interface, an additional (ponderomotive) force arises, inducing an electroosmotic moisture flux j_3 toward Surface 2. Under the action of the electric field, a directed movement of electric charges in the diffuse part of the electrical double layer occurs, accompanied by the movement of the liquid layer along the pore surfaces (electroosmosis) [34, 35].

If a well-permeable wet medium is present on the side of Surface 2, a significant portion of moisture is absorbed into the porous layer through capillary imbibition. Capillary imbibition, driven by the gradient of capillary pressure, results in the formation of a filtration flux j_2.

As a result of the combined action of these fluxes, changes in the relative moisture content of the porous layer occur. Notably, if the dispersion of pore sizes in the porous body model is neglected, the relative moisture content α_m, defined as before, coincides with the phase interface boundary:

$$\bar{z}_m = \frac{L_m}{L_0}.$$

The mass of liquid lost during the drying process is given by:

$$\Delta m = m_{Ln} - m_L = \Pi S \rho_L L_0 \left(1 - \bar{z}_m\right),$$

where S is the pore area; ρ_L is the density of water; Π is the porosity of the material. Given that the rate of change of liquid mass in the layer is determined by the vapor and liquid flux j from the layer, let's arrive at the differential equation governing the relative moisture content α_m in the layer, which can also be interpreted as the equation of motion for the phase interface:

$$\frac{d\alpha_m}{dt} = \frac{d\bar{z}_m}{dt} = -\frac{j\left(\bar{z}_m\right)}{\Pi \rho_L L_0},$$

where $j\left(\bar{z}_m\right)$ is the total flux acting in the porous medium, which is the sum of the vapor flux, the electroosmotic flux, and the flux induced by capillary pressure, counteracting the electroosmotic flow.

The phase transition from liquid to vapor at the gas-liquid interface is accounted for by specifying the density of the saturating vapor on this surface, which depends on the temperature and is given by the formula:

$$\rho_n(T) = 133e^{\left[18.681-\frac{4105}{(T-35)}\right]}\frac{M_v}{RT}\ \left(\text{kg/m}^3\right). \tag{4.20}$$

As a result of solving the nonlinear boundary problem, the dependence of the convective-diffusive vapor flux on the parameters of the porous and boundary layers is determined in the form [30, 39]:

$$j_1\left(\bar{z}_m\right) = \frac{\Omega}{B-\Gamma_0\bar{z}_m}, \tag{4.21}$$

where Ω is a parameter characterizing the intensity of moisture transfer, which depends on the physical properties of the medium and the drying conditions; B is a coefficient that depends on the effective diffusion and permeability characteristics of the porous medium; Γ_0 is a parameter characterizing the influence of the electric field on the mass transfer process [2].

4.1.1 CAPILLARY MOISTURE FLOW

The transfer caused by capillary imbibition is considered. The capillary pressure is determined by the Laplace equation:

$$P_k = P_L - P_g = \frac{-2\sigma_{Lg}\cos\theta}{\bar{R}},$$

where θ is the angle formed by the meniscus surface with the solid surface; P_L, P_g are the pressures in the liquid and gas phases, respectively; σ_{Lg} is the surface tension coefficient at the liquid-gas interface.

In the Laplace equation, $\bar{R}$ represents the equivalent Kelvin radius. The flux j_2 caused by capillary imbibition is determined using Poiseuille's equation:

$$j_2 = \Pi\rho_L\frac{K_L}{\mu_L}\frac{P_K}{L_0\bar{z}_m}, \tag{4.22}$$

where K_L is the permeability of the liquid; μ_L is the dynamic viscosity of the liquid.

4.1.2 ELECTROOSMOTIC LIQUID FLOW

The liquid flow caused by the action of an external constant electric field is considered under the condition of the presence of a dried pore zone. The effect of the electric field on the pore liquid is associated with the presence of a double electric layer near the pore surface. The skeleton material is assumed to be hydrophilic, and the minimum transverse pore size is significantly larger than the thickness of the diffuse part of the double electric layer $\delta_e = 1/K_e$, where for a symmetric binary electrolyte solution [1, 32]:

$$K_e = \sqrt{2\pi F_f^2 Z^2 C_0 / \varepsilon^{(1)} RT},$$

where F_f is Faraday's constant; Z is valence of ions considering their charge sign; C_0 is electrolyte solution concentration; $\varepsilon^{(1)}$ is absolute dielectric permeability of the liquid.

Then, on average, the charge density ρ_e in the diffuse part of the double electric layer is determined as [1]:

$$\rho_e = \rho_{e0} e^{-K_e\left(\bar{R}-r\right)}, \tag{4.23}$$

where ρ_{e0} is charge density value on the surface of capillaries; r is running radial coordinate.

For the assumed condition of the smallness of the double electric layer thickness compared to the capillary radius, $K_e\bar{R} >> 1$.

The force density across the capillary section:

$$f_e = \rho_e E_L,$$

where $E_L = U_L/L_m$ is electric field intensity; U_L is voltage applied to the liquid-filled part of the capillary.

The average force density:

$$\bar{f}_e = \frac{2\rho_{e0}E_L}{K_e\bar{R}} - \frac{2\rho_{e0}E_L}{(K_e\bar{R})^2}(1 - e^{-K_e\bar{R}}).$$

For the earlier assumption $\bar{R}K_e >> 1$, let's obtain:

$$\bar{f}_e \approx \frac{2\rho_{e0}E_L}{K_e\bar{R}} = \frac{2\bar{\eta}E_L}{\bar{R}},$$

where $\bar{\eta} = \rho_{e0} / K_e$.

The force acting on the charge in the capillary:

$$\bar{F}_e = \bar{f}_e S L_m.$$

The average pressure caused by electrical forces:

$$\bar{P}_e = \bar{F}_e / S = \bar{f}_e L_m.$$

The gradient of this pressure:

$$\vec{\nabla}\bar{P}_e = \left(d\bar{P}_e / dz\right)\vec{e}_z,\ d\bar{P}_e / dz = -\bar{P}_e / L_m = -\bar{F}_e / SL_m = -\bar{f}_e.$$

Considering that the current forces I_g and I_L in the dried and liquid-saturated pore regions are equal, i.e., $I_g = I_L$, according to Ohm's law:

$$I_g = U_g / R_g,\ I_L = U_L / R_L,$$

let's obtain $U_g / U_L = R_g / R_L$.

Here

$$R_g = \rho_g^*(L_0 - L_m) / S,\ R_L = \rho_L^* L_m / S,$$

where ρ_g^*, ρ_L^* are the specific resistances of these regions.

As the voltage U between the layer surfaces is $U = U_g + U_L$, then:

$$\frac{U}{U_L} = 1 + \frac{\rho_g^*\left(1 - \bar{z}_m\right)}{\rho_L^* \bar{z}_m} = 1 + \frac{\left(1 - \bar{z}_m\right)}{\varepsilon_\rho \bar{z}_m}. \tag{4.24}$$

Here $\varepsilon_\rho = \rho_L^* / \rho_g^*$ is the ratio of specific resistances in the liquid and dried zones, and $\bar{z}_m = L_m / L_0$. From (4.24), it follows that:

$$U_L = \varepsilon_\rho U \bar{z}_m / \left[(1 - \bar{z}_m) + \varepsilon_\rho \bar{z}_m\right].$$

Then the electric field intensity in the liquid zone is:

$$E_L = U_L / L_m = \varepsilon_\rho U / L_0\left[(1 - \bar{z}_m) + \varepsilon_\rho \bar{z}_m\right].$$

The formulas for determining the pressure gradient and the magnitude of the electroosmotic flow j_3 are given as follows:

$$\frac{d\bar{P}_e}{dz} = -\bar{f}_e = -\frac{2\bar{\eta}}{\bar{R}}\frac{\varepsilon_\rho U}{L_0\left[\varepsilon_\rho \bar{z}_m + (1-\bar{z}_m)\right]};$$

$$j_3 = \Pi \rho_L \upsilon_3;$$

$$\upsilon_3 = \frac{K_L}{\mu_L}\frac{dP_e}{dz} = -\frac{K_L}{\mu_L}\frac{2\bar{\eta}}{\bar{R}}\frac{\varepsilon_\rho U}{L_0\left[\varepsilon_\rho \bar{z}_m + \left(1-\bar{z}_m\right)\right]}. \tag{4.25}$$

4.1.3 SOLUTION OF THE PROBLEM AND RESULTS OF QUANTITATIVE ANALYSIS

The determination of the change in relative moisture content during the drying process is reduced to the Cauchy problem, where the convective-diffusion flow is determined from (4.21), and the capillary and electroosmotic flows are determined from (4.22) and (4.23), respectively:

$$\frac{d\bar{z}_m}{dt} = -\frac{\Omega}{B-\Gamma_0\bar{z}_m} + \frac{\tilde{K}}{\bar{z}_m} + \frac{\tilde{K}_1}{\left(1-\bar{z}_m\right)+K_2\bar{z}_m},\ \bar{z}_m\left(0\right)=1; \tag{4.26}$$

$$\tilde{K} = \frac{K_L}{\mu_L \bar{R}}\frac{2\sigma_{Lg}}{L_0^2},\ \tilde{K}_1 = \frac{K_L}{\mu_L}\frac{2\bar{\eta}\varepsilon_\rho E}{\bar{R}L_0}.$$

Equation (4.26) can be written as follows:

$$\frac{a_{32}\bar{z}_m^3 + a_{22}\bar{z}_m^2 + a_{12}\bar{z}_m}{a_{21}\bar{z}_m^2 + a_{11}\bar{z}_m + a_{01}}\frac{d\bar{z}_m}{dt} = 1;$$

where

$$a_{21} = \Omega(1-K_2) + \tilde{K}\Gamma_0(1-K_2) - \tilde{K}_1\Gamma_0;$$

$$a_{11} = -\Omega - \tilde{K}B(1-K_2) - \tilde{K}\Gamma_0 + \tilde{K}_1 B;$$

$$a_{01} = \tilde{K}B;\ \ a_{32} = \Gamma_0(1-K_2);$$

$$a_{22} = -B(1-K_2) - \Gamma_0;$$

$$a_{12} = B;$$

or

$$\left[\frac{a_{32}}{a_{21}}\frac{\bar{z}_m}{2} + \frac{a_{42}\bar{z}_m^2 + a_{41}\bar{z}_m}{a_{21}\bar{z}_m^2 + a_{11}\bar{z}_m + a_{01}}\right]d\bar{z}_m = dt;$$

$$a_{42} = a_{22} - \frac{a_{32}a_{11}}{a_{21}};$$

$$a_{41} = a_{12} - \frac{a_{32}a_{01}}{a_{21}}.$$

The solution of (4.26) using the initial condition $\bar{z}_m(0) = 1$ has the form:

$$\frac{1}{2}\frac{a_{32}}{a_{21}}\left(\bar{z}_m^{\,2} - 1\right) + \frac{a_{42}}{a_{21}}\left(\bar{z}_m - 1\right) + \left(-\frac{a_{42}a_{11}}{2a_{21}^2} + \frac{a_{41}}{2a_{21}}\right)\ln\left|f_2\left(\bar{z}_m\right)\right| + f\left(\bar{z}_m\right) = t, \qquad (4.27)$$

where

$$f(\bar{z}_m) = \left(\frac{a_{42}(a_{11}^2 - 2a_{21}a_{01})}{2a_{21}^2} - \frac{a_{41}a_{11}}{2a_{21}}\right) f_1(\bar{z}_m);$$

$$f_1(\bar{z}_m) = \frac{2}{\sqrt{4a_{21}a_{01} - a_{11}^2}}\left(\arctan\frac{2a_{21}\bar{z}_m + a_{11}}{\sqrt{4a_{21}a_{01} - a_{11}^2}} - \arctan\frac{2a_{21} + a_{11}}{\sqrt{4a_{21}a_{01} - a_{11}^2}}\right);$$

$$\left|f_2(\bar{z}_m)\right| = \left|\frac{a_{21}\bar{z}_m^2 + a_{11}\bar{z}_m + a_{01}}{a_{21} + a_{11} + a_{01}}\right|, \text{ if } 4a_{21}a_{01} > a_{11}^2.$$

Otherwise,

$$f_1(\bar{z}_m) = \frac{1}{\sqrt{a_{11}^2 - 4a_{21}a_{01}}}\ln\left|f_3(\bar{z}_m)\right|,$$

where

$$f_3(\bar{z}_m) = \frac{2a_{21}\bar{z}_m + a_{11} - \sqrt{a_{11}^2 - 4a_{21}a_{01}}}{2a_{21}\bar{z}_m + a_{11} + \sqrt{a_{11}^2 - 4a_{21}a_{01}}}\,\frac{2a_{21} + a_{11} + \sqrt{a_{11}^2 - 4a_{21}a_{01}}}{2a_{21} + a_{11} - \sqrt{a_{11}^2 - 4a_{21}a_{01}}}, \text{ if } a_{11}^2 > 4a_{21}a_{01}.$$

The formulas obtained above are the basis for a quantitative analysis of the influence of geometric and physical parameters on the drying a porous layer of cement stone.

Table 4.1 shows the dependence of relative moisture content at a fixed point in time on temperature and boundary layer thickness during capillary infiltration under natural drying (without an electric field). The influence of an external constant electric field is illustrated by the data given in **Tables 4.2** and **4.3** for different boundary layer thicknesses.

Table 4.1 Consideration of capillary imbibition ($t = 10^4$ s, $L_0 = 0.1$ m)

	δ, m	$T_1 = 300$ K	$T_2 = 310$ K	$T_3 = 320$ K	$T_4 = 330$ K
$\alpha_m = \bar{z}_m$	0.0001	0.573	0.428	0.254	0.082
	0.001	0.591	0.445	0.27	0.091
	0.01	0.727	0.59	0.416	0.209
	0.1	0.967	0.933	0.875	0.784

Table 4.2 Influence of electric field intensity on relative moisture content at $E = 200$ V/m

	δ, m	$T_1 = 300$ K	$T_2 = 310$ K	$T_3 = 320$ K	$T_4 = 330$ K
$\alpha_m = \bar{z}_m$	0.0001	0.561	0.415	0.242	0.075
	0.001	0.577	0.432	0.257	0.083
	0.01	0.705	0.569	0.396	0.193
	0.1	0.914	0.873	0.81	0.718

Table 4.3 Influence of electric field intensity on relative moisture content at $E = 400$ V/m

	δ, m	$T_1 = 300$ K	$T_2 = 310$ K	$T_3 = 320$ K	$T_4 = 330$ K
$\alpha_m = \bar{z}_m$	10^{-4}	0.524	0.377	0.206	0.059
	10^{-2}	0.647	0.511	0.343	0.149

In **Fig. 4.1** and **4.2**, the dynamics of relative moisture content dependence on time are shown for $\delta = 0.001$ m and $\delta = 0.1$ m, respectively (curves 1, 2, 3, 4) for $T = 300$ K, 310 K, 320 K, and 330 K.

From the provided quantitative data, it follows that the intensity of drying significantly depends on the thickness of the boundary layer. When the thickness of the boundary layer increases by a factor of 100, the relative moisture content may increase by a factor of 10 or more. At a boundary layer thickness of $\delta = 0.1$ m and temperatures of 300 K, 310 K, and 320 K, the relative moisture content decreases by no more than 10 % over approximately 3 hours.

An electric field intensity of $E = 200$ V/m and $E = 400$ V/m (these are not high fields) counteracts liquid infiltration through wall 2, leading to a resultant reduction in relative moisture content of up to 40 %.

Let's investigate the influence of electroosmosis on the drying process of a porous layer under convective mass transfer on one of its surfaces. Let's consider a porous layer initially saturated with moisture, where one surface (Surface 1) is in contact with a gaseous environment (air), while the other surface (Surface 2) is in contact with a moisture-saturated, highly permeable wet medium. It is assumed that gas flow can be applied to Surface 1 and a constant difference in electric potential can be created between Surfaces 1 and 2. This allows to explore the possibility of stimulating and controlling the drying process through air blowing on Surface 1 and electroosmotic moisture removal. The transport of air and vapor in the dried region is described by the Stefan-Maxwell equations [31] with boundary conditions on Surface 1.

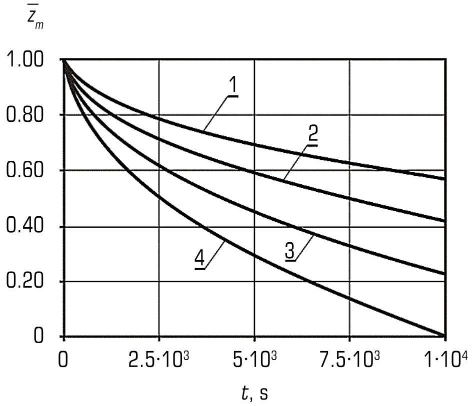

Fig. 4.1 Dependence of relative moisture content on time at different temperatures for $\delta = 0.001$ m

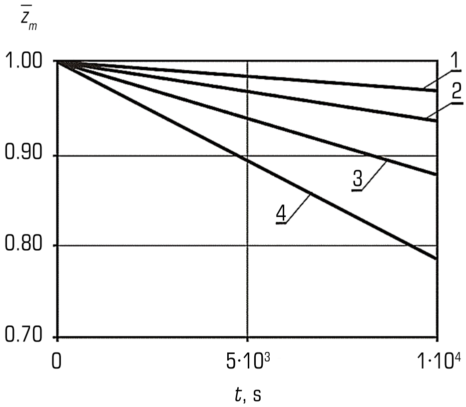

Fig. 4.2 Dependence of relative moisture content on time at different temperatures for $\delta = 0.1$ m

4.2 ENHANCEMENT OF CONVECTIVE DRYING OF A POROUS LAYER SURFACE BY ELECTROOSMOSIS

Solving the nonlinear boundary value problem, let’s determine the vapor density at the wall η_1 and the vapor flux magnitude j_1:

$$\eta_1 = -\left(A + B\bar{z}_m^*\right) + \sqrt{U + S\bar{z}_m^* + B^2\bar{z}_m^{*2}}, \tag{4.28}$$

$$j_1 = H\left[-\left(a_1 + B\bar{z}_m^*\right) + \sqrt{U + S\bar{z}_m^* + B^2\bar{z}_m^{*2}}\right]. \tag{4.29}$$

Due to the pressure effect under the meniscus of the water surface in the pores at the gas-liquid contact boundary, capillary moisture inflow occurs from the medium in contact with the layer at Surface 2. The competition between drying and moisture inflow may lead to a steady-state moisture content level in the layer. To further reduce moisture, a constant electric field generated by an external source can be used. The action of the field on the electric charge in the diffuse part of the double electric layer at the solid-liquid interface creates an additional (ponderomotive) force that reduces moisture inflow or drives electroosmotic moisture flux toward Surface 2. The vapor outflow conditions through Surface 1 of the drying body are modeled using third-kind mass transfer conditions (4.29). The mass transfer coefficient is related to the nature of the air blowing on Surface 1, which intensifies the drying process.

The total flux j consists of the diffusion-convective flux j_1, the flux due to capillary imbibition j_2, and the electroosmotic liquid flux j_3, caused by the force with which the electric field acts on the charged liquid.

For partial filling of the capillary with liquid, surface forces act at the three-phase liquid-gas-solid interface, forming a meniscus – a curved gas-liquid boundary surface.

The flux j_2 due to capillary imbibition, according to Poiseuille’s equation, is defined as:

$$j_2 = \Pi\rho_L v_L = \Pi\rho_L \frac{K_L}{\mu_L}\frac{P_K}{L_0\left(1-\bar{z}_m^*\right)}. \tag{4.30}$$

The electroosmotic flux is given in the form:

$$j_3 = \rho_L v_{osm}\Pi = \frac{\rho_L K_L \Pi}{\mu_L}\frac{2\bar{\eta}\varepsilon_\rho E}{\bar{R}\left[\left(1-\bar{z}_m\right)+\varepsilon_\rho \bar{z}_m\right]}. \tag{4.31}$$

Thus, the problem reduces to the following Cauchy problem:

$$\frac{d\bar{z}_m^*}{dt} = H\left[f\left(\bar{z}_m^*\right) + \frac{\tilde{K}}{1-\bar{z}_m^*} + \frac{\tilde{K}_1}{K_2\left(1-\bar{z}_m^*\right) + K_3\bar{z}_m^*}\right],\ H = -\frac{\beta\rho_n}{\Pi\rho_0\rho_L}; \tag{4.32}$$

$$f\left(\bar{z}_m^*\right) = -\left(a_1 + B\bar{z}_m^*\right) + \sqrt{U + S\bar{z}_m^* + B^2\bar{z}_m^{*2}}, \tag{4.33}$$

under the initial condition $\bar{z}_m^*(0) = 0$,

where $\tilde{K} = \frac{\rho_L K_L P_k}{\mu_L L_0 \beta\rho_n}$; $P_k = -\frac{2\sigma}{\bar{R}}$; $K_2 = \varepsilon_\rho$; $K_3 = 1$; $\tilde{K}_1 = \frac{2K_L\rho_L\Pi\varepsilon_\rho\bar{\eta}E}{\beta\rho_n\mu_L\bar{R}}$.

By substituting the variables $\sqrt{U + S\bar{z}_m^* + B^2\bar{z}_m^{*2}} = \chi + \bar{z}_m^* B$, (4.33) transforms into:

$$-\frac{2\left(B\chi^2 - S\chi + BU\right)}{\left(S - 2B\chi\right)^2}\frac{d\chi}{dt} = H\left(\chi - a_1\right)f_2\left(\chi\right), \tag{4.34}$$

$$f_2\left(\chi\right) = \frac{\left(\tilde{a}\chi^4 + \tilde{b}\chi^3 + c\chi^2 + \tilde{d}\chi + \tilde{e}\right)}{\left(\chi^2 + 2\chi B - \omega_1\right)\left(\Omega_2\chi^2 + \Omega_1\chi + \Omega_0\right)}, \tag{4.35}$$

where

$$\omega_1 = S + U;$$

$$\Omega_2 = K_2 - K_3;$$

$$\Omega_1 = 2K_2 B;$$

$$\Omega_0 = -K_2\omega_1 + K_3 U;$$

$$\tilde{a} = 1;$$

$$\tilde{b} = \frac{\Omega_1 + 2B\Omega_2}{\Omega_2};$$

$$\tilde{c} = \frac{\Omega_0 + 2B\Omega_1 - \Omega_2\omega_1 + 2\tilde{K}B\Omega_2 + 2\tilde{K}_1 B}{\Omega_2};$$

$$\tilde{e} = \frac{2\tilde{K}B\Omega_0 - \Omega_0\omega_1 - 2\tilde{K}_1 B\omega_1}{\Omega_2};$$

$$\tilde{d} = \frac{2B\Omega_0 - \Omega_1\omega_1 + 2\tilde{K}B\Omega_1 + 4\tilde{K}_1 B^2}{\Omega_2}. \tag{4.36}$$

Equation (4.34) can be rewritten as:

$$-\frac{2\left(B\chi^2-S\chi+BU\right)f_3(\chi)}{\left(S-2B\chi\right)^2\left(\chi-a_1\right)f_4(\chi)}\frac{d\chi}{dt}=H\Omega_2, \tag{4.37}$$

$$f_3(\chi)=\left(\chi^2+2\chi B-\omega_1\right)\left(\Omega_2\chi^2+\Omega_1\chi+\Omega_0\right),$$

$$f_4(\chi)=\left(\chi-c_1\right)\left(\chi-c_2\right)\left(\chi-c_3\right)\left(\chi-c_4\right),$$

where $c_i=\chi_i$, $i=\overline{1,4}$ are the roots of the fourth-order polynomial appearing in the numerator of equation (4.35).

The solution to this equation, considering the initial condition $\overline{z}_m^*(0)=0,$ is given by:

$$D_1\ln\left|\frac{S-2B\chi}{S-2B\sqrt{U}}\right|+D_2\left[\frac{1}{S-2B\chi}-\frac{1}{S-2B\sqrt{U}}\right]+$$
$$+D_3\left[\frac{1}{(S-2B\chi)^2}-\frac{1}{(S-2B\sqrt{U})^2}\right]+R_3\ln\left|\frac{\chi-c_1}{\sqrt{U}-c_1}\right|+R_4\ln\left|\frac{\chi-c_2}{\sqrt{U}-c_2}\right|+$$
$$+R_5\ln\left|\frac{\chi-c_3}{\sqrt{U}-c_3}\right|+R_6\ln\left|\frac{\chi-c_4}{\sqrt{U}-c_4}\right|=H\Omega_2 t, \tag{4.38}$$

where $D_1=-\frac{R_2}{8B^3}$; $D_2=-\frac{1}{4B^2}\left(\frac{R_2S}{B}+R_1\right)$; $D_3=\frac{1}{4B}\left(\frac{R_2S^2}{4B^2}+\frac{R_1S}{2B}+R_0\right)$; and coefficients R_0, R_1, …, R_6 are solutions of the algebraic system:

$$\sum_{i=0}^{2}d_{i,6-j}R_i+\sum_{i=3}^{6}b_{i-2,6-j}R_i=4B\Omega_{1,6-j}\ \left(j=\overline{0,6}\right),$$

$$d_{0,6}=d_{16}=d_{05}=0;\ \ d_{2,6}=d_{1,5}=d_{0,4}=1;\ \ d_{2,5}=d_{1,4}=d_{0,3}=\tilde{b};$$

$$d_{2,4}=d_{1,3}=d_{0,2}=\tilde{c};\ \ d_{2,3}=d_{1,2}=d_{0,1}=\tilde{d};\ \ d_{2,2}=d_{1,1}=d_{0,0}=\tilde{e};$$

$$b_{i,6}=8B^3a_{i+2,3};$$

$$b_{i,5}=8Ba_{i+2,2}+12B^2Sa_{i+2,3},\ldots\ b_{i,4}=8B^3a_{i+2,1}+12B^2Sa_{i+2,2}-6BS^2a_{i+2,3};$$

$$b_{i,3}=8B^3a_{i+2,0}+12B^2Sa_{i+2,1}-6BS^2a_{i+2,2}+S^3a_{4,3};$$

$$b_{i,2} = 12B^2Sa_{i+2,0} - 6BS^2a_{i+2,1} + S^3a_{4,2},\ b_{i,1} = -6BS^2a_{i+2,0} + S^3a_{4,1};$$

$$b_{i,1} = S^3a_{4,0},\ a_{3,2} = -\left(c_4 + c_2 + c_3\right),\ a_{3,1} = \left(c_2 + c_3\right)c_4 + c_2c_3;$$

$$a_{3,0} = -c_2c_3c_4,\ a_{4,2} = -\left(c_4 + c_1 + c_3\right),\ a_{i+2,1} = 1,\ a_{4,1} = \left(c_1 + c_3\right)c_4 + c_1c_3;$$

$$a_{4,0} = -c_1c_3c_4;$$

$$a_{5,2} = -\left(c_2 + c_1 + c_4\right);\ a_{5,1} = \left(c_1 + c_2\right)c_4 + c_1c_2;\ a_{5,0} = -c_1c_4c_2;$$

$$a_{6,2} = -\left(c_2 + c_1 + c_3\right);\ a_{6,1} = \left(c_1 + c_2\right)c_3 + c_1c_2;\ a_{6,0} = -c_1c_3c_2;$$

$$a_{0,4} = B;\ a_{0,3} = 2B^2 - S;\ a_{0,2} = \omega_1B - 2BS + BU;\ a_{0,1} = \omega_1S + 2B^2U;$$

$$a_{0,0} = -BU\omega_1;\ \Omega_{16} = a_{0,4}\Omega_2;\ \Omega_{15} = a_{0,4}\Omega_1 + a_{0,3}\Omega_2;$$

$$\Omega_{14} = a_{0,4}\Omega_0 + a_{0,3}\Omega_1 + a_{0,2}\Omega_2,\ \Omega_{13} = a_{0,3}\Omega_0 + a_{0,2}\Omega_1 + a_{0,1}\Omega_2,$$

$$\Omega_{12} = a_{0,2}\Omega_0 + a_{0,1}\Omega_1 + a_{0,0}\Omega_2,\ \Omega_{11} = a_{0,1}\Omega_0 + a_{0,0}\Omega_1,\ \Omega_{10} = a_{0,0}\Omega_0.$$

The transcendental equation (4.38) establishes the relationship between the relative moisture content in the porous layer and time, depending on the system parameters, as presented in **Tables 4.4, 4.5**, and **Fig. 4.3–4.5**.

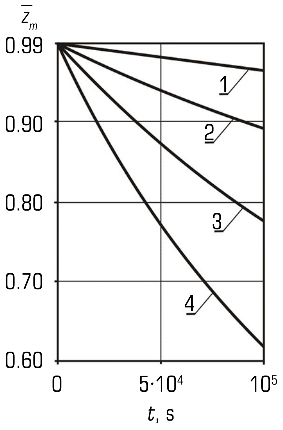

Fig. 4.3 Time variation of relative moisture content for different temperature values in the absence of an external electric field

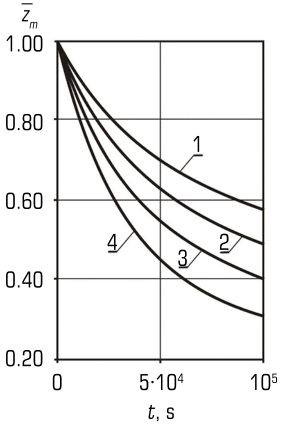

Fig. 4.4 Time variation of relative saturation as a function of temperature at a given electric field strength $E = 200$ V/m

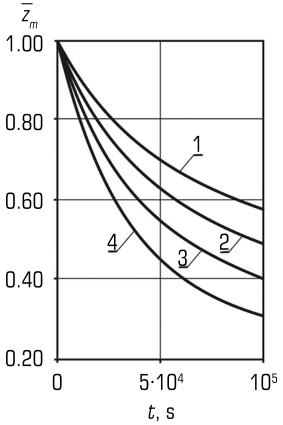

Fig. 4.5 Time dependence of relative moisture content for different values of the mass transfer coefficient at $E = 200$ V/m

4.2.1 NUMERICAL ANALYSIS OF PARAMETER INFLUENCE ON CONVECTIVE ELECTROOSMOTIC DRYING

Fig. 4.3–4.5 show the time dependence of relative moisture content considering capillary imbibition in the absence and presence of an external electric field. In **Fig. 4.3** and **4.4**, curves 1 correspond to a temperature of 300 K; curves 2 correspond to 310 K; curves 3 correspond to 320 K; curves 4 correspond to 330 K. The calculations were performed using $\beta = 0.01$ and $L_0 = 0.1$ m. The analysis of the results indicates that at $T = 300$ K, an electric field intensity of $E = 200$ V/m reduces the relative moisture content of the layer from 0.960 to 0.574 for $t = 10^6$ s, whereas at $T = 330$ K, it decreases from 0.620 to 0.313, nearly by a factor of two.

Table 4.4 Dependence of relative moisture content $\bar{z}_m = 1 - \bar{z}_m^*$ on temperature at a mass transfer coefficient $b = 0.01$ for $E = 200$ V/m, and $E = 400$ V/m

E, V/m	***T*, K**			
	300	**310**	**320**	**330**
200	0.574	0.488	0.397	0.312
400	0.395	0.319	0.261	0.222

Table 4.5 Dependence of relative moisture content $\bar{z}_m$ on the mass transfer coefficient b at $T = 300$ K, $E = 200$ V/m, and $E = 400$ V/m

E, V/m	β					
	0.01	**0.005**	**0.0025**	**0.001**	**0.0005**	**0.0001**
200	0.574	0.594	0.617	0.646	0.656	0.664
400	0.349	0.395	0.429	0.455	0.462	0.47

In **Fig. 4.4 and 4.5**, curves 1–6 correspond to the values of the mass transfer coefficient $\beta = 0.0001, 0.0005, 0.001, 0.0025, 0.005$, and 0.01. In **Fig. 4.4**, curves 1–4 almost coincide with the abscissa axis, indicating that the relative moisture content corresponding to these curves is approximately equal to one, meaning that the moisture content of the layer remains nearly unchanged over the studied time interval. In the presence of an external constant electric field (**Fig. 4.5**), the drying process of the layer becomes significantly more effective. The drying rate also increases with higher mass transfer coefficients and temperature.

4.3 INFLUENCE OF AN EXTERNAL CONSTANT ELECTRIC FIELD ON BILATERAL NATURAL DRYING OF A POROUS LAYER

A porous layer, initially saturated with moisture, is considered within a Cartesian coordinate system (x, y, z) and occupies the region $0 < z < L_0$. The layer undergoes mass exchange with the surrounding environment from both sides, while the temperature of the medium and the layer remains the same. A constant difference in electric potential is maintained between the surfaces of the layer. Due to the action of the field on the electric charge within the diffuse part of the electrical double layer near the solid matrix–pore liquid interface, an additional (ponderomotive) force arises, inducing an electroosmotic moisture flow within the body. The surface from which the electroosmotic flow is directed will be referred to as the first surface (Surface 1), while the other surface (toward which the flow is directed) will be referred to as Surface 2. The coordinate system is chosen such that Surface 1 coincides with $z = L_0$ and Surface 2 with $z = 0$.

As a result of liquid evaporation from the pores and vapor outflow to the external environment, a zone of dried pores forms on the side of Surface 1, filled with a mixture of air, vapor, and residual liquid bound to the pore surfaces, which remains stable against drying at a given temperature. During the drying process, this zone expands deeper into the material. Let's consider a class of materials with low permeability to liquids, where the influence of a two-phase zone can be neglected [1]. Therefore, the formation of two distinct zones is assumed: dried pores and liquid-filled pores. The boundary between these zones within each pore is marked by a liquid meniscus, the convexity or concavity of which is determined by the properties of the pore surface (its hydrophilicity or hydrophobicity).

4.3.1 MASS TRANSFER IN THE SURROUNDING GAS

When formulating the mass transfer problem in the surrounding gas, it is assumed that changes in the density of its components – air and vapor – occur only within a certain layer of thickness δ_i, $(i = 1,2)$, which occupies the regions $L_0 < z < L_0 + \delta_1$, $0 > z > -\delta_2$. At the surfaces $z = L_0 + \delta_1$, $z = -\delta_2$, the air and vapor densities are equal to their values in atmospheric air. Thus, the mass transfer problem in the surrounding gas includes:

– the Stefan-Maxwell equations [31]:

$$\frac{\partial \rho_{ae}}{\partial z} - \frac{\rho_{ae}}{D_1}\upsilon = 0, \quad \frac{\partial}{\partial z}\left(\frac{\partial \rho_{ve}}{\partial z} - \frac{\rho_{ve}}{D_1}\upsilon\right) = 0, \quad \frac{\rho_{ae}}{M_a} + \frac{\rho_{ve}}{M_v} = \frac{P_{g1}}{RT}, \tag{4.39}$$

in the regions $L_0 + \delta_1 > z > L_0$, $0 > z > -\delta_2$;

– the boundary conditions:

$$\frac{\rho_{ve1}}{M_v}\upsilon - \frac{D_1}{M_v}\frac{\partial \rho_{ve1}}{\partial z} = j_1(L_0, t) \text{ on the surface } z = L_0; \tag{4.40}$$

$$\rho_{ve} = \rho_{v1}, \quad \rho_{ae} = \rho_{a1}, \quad \rho_{a1} = \frac{M_a P_{g1}}{RT} - \frac{M_a}{M_v}\rho_{v1} \text{ on the surface } z = L_0 + \delta; \tag{4.41}$$

$$\frac{\rho_{ve2}}{M_v}\upsilon_2 - \frac{D_1}{M_v}\frac{\partial \rho_{ve2}}{\partial z} = j_2(0, t) \text{ on the surface } z = 0; \tag{4.42}$$

$$\rho_{ve2} = \rho_{v2}, \quad \rho_{ae2} = \rho_{a2}, \quad \rho_{a2} = \frac{M_a P_{g1}}{RT} - \frac{M_a}{M_v}\rho_{v2} \text{ on the surface } z = -\delta_2, \tag{4.43}$$

where ρ_{vei}, ρ_{aei} are the vapor and air densities, respectively; ρ_{vi}, ρ_{ai} are the vapor and air densities at the surfaces $z = L_0 + \delta_1$, $z = -\delta_2$; υ_i is the mass-averaged velocity; j_1, j_2 are the vapor fluxes at the surfaces.

4.3.2 MASS TRANSFER IN THE ZONE OF DRIED PORES

Mass transfer in the gas zone within the porous layer will also be described using the Stefan-Maxwell equations [31]. However, the gas pressure P in the pores depends on the coordinate, and the mass-averaged velocity υ satisfies Darcy's law. Then, the transport equations in the region $L_0 > z > L_{\max}$ take the form:

$$\rho_a \frac{K_g}{\mu_g}\frac{\partial P}{\partial z} + D\frac{\partial \rho_a}{\partial z} = 0, \quad \frac{\partial}{\partial z}\left(\rho_v \frac{K_g}{\mu_g}\frac{\partial P}{\partial z} + D\frac{\partial \rho_v}{\partial z}\right) = 0, \tag{4.44}$$

where $L_{\max}$ is the coordinate of the gas-liquid contact boundary within the porous layer.

The boundary conditions at the surfaces $z = L_0$ and $z = L_{\max}$ in the gas zone are given as follows:

$$\rho_v \frac{K_g}{\mu_g}\frac{\partial P}{\partial z} + D\frac{\partial \rho_v}{\partial z} = -j_1 \text{ on the surface } z = L_0; \tag{4.45}$$

$$\rho_v = \rho_n \text{ on the surface } z = L_{\max}. \tag{4.46}$$

When a zone of dried pores forms near Surface 2, the mass transfer in this region is described by equation (4.44) with the following boundary conditions:

$$\rho_v \frac{K}{\mu_g}\frac{\partial P}{\partial z} + D\frac{\partial \rho_v}{\partial z} = j_2 \text{ on the surface } z = 0,$$

$$\rho_v = \rho_n \text{ on the surface } z = L_{\min}. \tag{4.47}$$

Equations (4.39)–(4.48) form a complete system of relationships for determining the convective-diffusive vapor flux in the given porous layer. The expression for this flux is obtained in the form:

$$j_1(\bar{z}_m) = \frac{\Omega}{B - \Gamma_0 \bar{z}_m}, \tag{4.48}$$

where $\bar{z}_m$ is relative moisture content of the porous layer; B is a coefficient characterizing the convective-diffusive transfer equation, which includes material and transport properties; Γ_0 is a coefficient accounting for the influence of relative moisture content $\bar{z}_m$ on mass transfer; C_0 is initial concentration of moisture; $\eta_0 = \frac{\rho_{v1}}{\rho_n}$ is a dimensionless parameter expressing the ratio of vapor density ρ_{v1} to a reference density ρ_n; a, b are coefficients of porosity and diffusion properties, respectively.

The electroosmotic flow is described by equation (4.25):

$$j_3 = \Pi\rho_L\upsilon_{3}, \quad \upsilon_3 = \frac{K_L}{\mu_L}\frac{dP_e}{dz} = -\frac{K_L}{\mu_L}\frac{2\bar{\eta}}{\bar{R}}\frac{\varepsilon_\rho U}{L_0\left[\varepsilon_\rho \bar{z}_m + \left(1-\bar{z}_m\right)\right]}. \tag{4.49}$$

4.3.3 LIQUID FLOW UNDER THE INFLUENCE OF CAPILLARY FORCES

Let the electric forces be sufficiently strong so that the liquid flows out through Surface 2. In this case, the capillary pressure $P_k = P_L - P = 2\sigma Lg\cos\theta / \bar{R}$ induces a flow of liquid j_4 in the direction opposite to the electroosmotic flow:

$$j_4 = \Pi\rho_L\upsilon_4, \quad \upsilon_4 = \frac{K_L}{\mu_L}\frac{P_K}{L_{\max}} = \frac{K_L}{\mu_L}\frac{P_K}{L_0\bar{z}_m}\,. \tag{4.50}$$

The total liquid flux j_L is determined as the sum of fluxes j_3 and j_4:

$$j_L = j_3 + j_4 = \Pi\rho_L\frac{K_L}{\mu_L}\left(\frac{P_K}{L_0\bar{z}_m} - \frac{2\bar{\eta}}{\bar{R}}\frac{\varepsilon_\rho U}{L_0\left[\varepsilon_\rho \bar{z}_m + \left(1-\bar{z}_m\right)\right]}\right). \tag{4.51}$$

During electroosmotic displacement of liquid through Surface 2 (i.e., reduction of parameter $\bar{z}_m$), the magnitude of the first term in equation (4.52) will increase, while the second term changes weakly due to the smallness of parameter $\varepsilon_{\rho,}$ or even decreases (Stage 1). The total liquid flux through Surface 2 will decrease until it reaches zero. At this moment, the electric field can be switched off. The capillary pressures at surfaces $z = L_{\max}$ and $z = 0$ will equalize, and the pore liquid will reach equilibrium. Drying of the layer through Surface 2 will then commence, governed by equations (4.39), (4.42), (4.45), (4.47), and (4.48).

Thus, the acceleration of the drying process due to electroosmosis will be observed only during the first stage.

Setting the total liquid flux j_L to zero in equation (4.51), let's obtain the following expression for the parameter $\bar{z}_m^*$, which defines the thickness of the saturated layer at the transition from the first to the second drying stage:

$$\bar{z}_m^* = \frac{\sigma}{\sigma\left(1-\varepsilon_\rho\right)+\bar{\eta}\varepsilon_\rho U}. \tag{4.51}$$

Expression (4.51) is written for a zero wetting angle.

4.3.4 MASS BALANCE EQUATION FOR LIQUID

The rate of liquid reduction in the layer is determined by the fluxes of liquid and vapor from the body. For the first drying stage, the mass balance equation for the liquid can be written as:

$$\frac{dm}{dt} = -\Pi\left(j_1 - j_L\right)S. \tag{4.52}$$

Considering that for the first drying stage $m = \Pi S\rho_L L_m = \Pi S\rho_L L_0 \bar{z}_m$, equation (4.54) can be rewritten in terms of the parameter $\bar{z}_m$ as:

$$\frac{d\bar{z}_m}{dt} = -\frac{1}{L_0\rho_L}\left(j_1 - j_L\right), \tag{4.53}$$

with the initial condition:

$$\bar{z}_m = 1 \text{ at } t = 0. \tag{4.54}$$

The final value of the parameter $k_m = k_m^*$ corresponds to the first drying stage.

It is noteworthy that the relative moisture content $\alpha_m = m_z / m_0$ of the porous layer (m_z being the residual moisture mass in the layer after drying, and m_0 the initial moisture mass) during the first stage is determined by the parameter $\bar{z}_m$, i.e.:

$$\alpha_m = \bar{z}_m. \tag{4.55}$$

Indeed, using the definitions $m_z = \Pi S\rho_L L_{\max} = \Pi S\rho_L L_0 \bar{z}_m$ and $m_0 = \Pi S\rho_L L_0$, let's obtain the expression $\alpha_m = m_z / m_0$ for relative moisture content.

For the second drying stage, the mass balance equation takes the form:

$$\frac{dm}{dt} = -\Pi\left(j_1 - j_2\right)S, \tag{4.56}$$

with the initial condition:

$$m = \Pi S \rho_L L_0 \tilde{\bar{z}}_m^* \text{ at } t = t^*. \tag{4.57}$$

Here, t^* represents the time at which the parameter $\bar{z}_m$ reaches its final value $\tilde{\bar{z}}_m^*$ in the first drying stage.

The relative moisture content in this stage is given by:

$$\alpha_m = \frac{\left(L_{\max} - L_{\min}\right)}{L_0} = \left(\bar{z}_m - \bar{z}_{m1}\right), \tag{4.58}$$

where $L_{\min} = L_0 \bar{z}_{m1}$ is the coordinate of the boundary between the dried and saturated zones on Surface 2 of the porous layer. Since the change in the moisture mass of the layer is now determined by:

$$\Delta m = \Delta m_1 + \Delta m_2, \quad \Delta m_1 = \Pi S \rho_L \left(\tilde{\bar{z}}_m^* - \bar{z}_m\right), \quad \Delta m_2 = \Pi S \rho_L \bar{z}_{m1}, \tag{4.59}$$

where the change Δm_1 (change in $\bar{z}_m$) is governed by the vapor flux j_1, and Δm_2 (change in $\bar{z}_{m1}$) is governed by the flux j_2, the problem (4.56), (4.57) can be formulated as two Cauchy problems:

$$\frac{d\bar{z}_m}{dt} = -\frac{j_1}{L_0 \rho_L}, \tag{4.60}$$

under the initial condition:

$$\bar{z}_m = \bar{z}_m^* \text{ at } t = t^*; \tag{4.61}$$

and

$$\frac{d\bar{z}_{m1}}{dt} = \frac{j_2}{L_0 \rho_L}, \tag{4.62}$$

under the initial condition:

$$\bar{z}_{m1} = 0 \text{ at } t = t^*. \tag{4.63}$$

The relative moisture content is now determined by the formula $\alpha_m = \bar{z}_m - \bar{z}_{m1}$, and the drying process is completed when the condition $\bar{z}_m = \bar{z}_{m1}$ is met (i.e., $\alpha_m = 0$).

3.5 SOLUTION OF THE PROBLEM AND ANALYSIS OF THE OBTAINED RESULTS

The convective-diffusive fluxes j_1 and j_2 are determined from the solutions of problems (4.39)–(4.41), (4.44)–(4.46) and (4.39), (4.42)–(4.44), (4.47), (4.48) and are given by [40]:

$$j_1\left(\bar{z}_m\right)=\frac{\Omega_1}{B_1-\Gamma_{01}\bar{z}_m},\quad j_2\left(\bar{z}_{m1}\right)=\frac{\Omega_2}{B_2-\Gamma_{02}\bar{z}_{m1}}, \tag{4.64}$$

where for $i=1,2$:

$$\Omega_i=\left\{b_i\left[1+\frac{b_i}{2\left(1+a_i\right)}\right]-\left(C_{0i}-1\right)\left[1+\frac{C_{0i}-1}{2\left(1+a_i\right)}\right]\right\}\frac{DM_vP}{RT\delta_i},$$

$$B_i=1+\frac{C_{0i}-1}{1+a_i}+\Gamma_{0i},$$

$$C_{0i}=\frac{P_{g1}}{RT}\frac{M_a}{\rho_{ai}}=1+\frac{\rho_{vi}}{M_v}\frac{M_a}{\rho_{ai}},\quad a_i=\frac{D'M_a}{\left(\frac{K_g}{\mu_g}\right)\rho_{ai}RT},\quad b_i=\frac{\rho_nM_a}{\rho_{ai}M_v},\quad \Gamma_{0i}=C_{0i}\frac{L_0}{\delta_i}\frac{D_1'}{D'}.$$

Using expression (4.52) for the liquid flux in the layer and formula (4.64) for the flux j_1, the Cauchy problem (4.55), (4.56) for the first drying stage is formulated as:

$$\frac{d\bar{z}_m}{dt}=-\frac{\Omega_1}{B_1-\Gamma_{01}\bar{z}_m}+\frac{\tilde{K}}{\bar{z}_m}+\frac{\tilde{K}_1}{\left(1-\bar{z}_m\right)+K_2\bar{z}_m}\ \text{at}\ \bar{z}_m\left(0\right)=1, \tag{4.65}$$

where

$$\tilde{K}=\frac{K_L}{\mu_L\bar{R}}\frac{2\sigma_{Lg}}{L_0},\quad \tilde{K}_1=\frac{K_L}{\mu_L}\frac{2\bar{\eta}\varepsilon_\rho E}{\bar{R}},\quad K_2=\varepsilon_\rho.$$

Equation (4.65) can be rewritten as:

$$\frac{a_{32}\bar{z}_m^3+a_{22}\bar{z}_m^2+a_{12}\bar{z}_m}{a_{21}\bar{z}_m^2+a_{11}\bar{z}_m+a_{01}}\frac{d\bar{z}_m}{dt}=1, \tag{4.66}$$

where

$$a_{21}=\Omega_1\left(1-K_2\right)+\tilde{K}\Gamma_{01}\left(1-K_2\right)-\tilde{K}_1\Gamma_{01},\quad a_{11}=-\Omega_1-\tilde{K}B_1\left(1-K_2\right)-\tilde{K}\Gamma_{01}+\tilde{K}_1B_1,$$

$$a_{32} = \Gamma_{01}(1-K_2), \quad a_{22} = -B_1(1-K_2) - \Gamma_{01}, \quad a_{12} = B_1.$$

The solution of equation (4.65) with the initial condition (3.18) is given by:

$$\frac{1}{2}\frac{a_{32}}{a_{21}}\left(\bar{z}_m^2 - 1\right) + \frac{a_{42}}{a_{21}}\left(\bar{z}_m - 1\right) + \left(-\frac{a_{42}a_{11}}{2a_{21}^2} + \frac{a_{41}}{2a_{21}}\right)\ln\left|\phi\left(\bar{z}_m\right)\right| + f\left(\bar{z}_m\right) = t, \tag{4.7}$$

where

$$a_{42} = a_{22} - \frac{a_{32}a_{11}}{a_{21}}, \quad a_{41} = a_{12} - \frac{a_{32}a_{01}}{a_{21}}, \quad \phi\left(\bar{z}_m\right) = \frac{a_{21}\bar{z}_m^2 + a_{11}\bar{z}_m + \bar{z}_{01}}{a_{21} + a_{11} + a_{01}},$$

$$f\left(\bar{z}_m\right) = \left(\frac{a_{42}\left(a_{11}^2 - 2a_{21}a_{01}\right)}{2a_{21}^2} - \frac{a_{41}a_{11}}{2a_{21}}\right) f_1\left(\bar{z}_m\right),$$

$$f_1\left(\bar{z}_m\right) = \frac{2}{\sqrt{4a_{21}a_{01} - a_{11}^2}}\left(arctg\frac{2a_{21}\bar{z}_m + a_{11}}{\sqrt{4a_{21}a_{01} - a_{11}^2}} - arctg\frac{2a_{21} + a_{11}}{\sqrt{4a_{21}a_{01} - a_{11}^2}}\right), \text{ if } 4a_{21}a_{01} > a_{11}^2;$$

$$f_1\left(\bar{z}_m\right) = \frac{1}{\sqrt{a_{11}^2 - 4a_{21}a_{01}}}\ln\left|\frac{f_3\left(\bar{z}_m\right)}{f_3(1)}\right|, \text{ if } a_{11}^2 > 4a_{21}a_{01};$$

$$f_3\left(\bar{z}\right) = \frac{2a_{21}\bar{z} + a_{11} - \sqrt{a_{11}^2 - 4a_{21}a_{01}}}{2a_{21}\bar{z} + a_{11} + \sqrt{a_{11}^2 - 4a_{21}a_{01}}}.$$

The transcendental Eq. (4.67) provides the dependence of relative moisture content in the porous layer on time during the first drying stage. The final moment t^* of the first stage is given by:

$$t^* = \frac{1}{2}\frac{a_{32}}{a_{21}}\left[\left(\bar{z}_m^*\right)^2 - 1\right] + \frac{a_{42}}{a_{21}}\left(\bar{z}_m^* - 1\right) + \left(-\frac{a_{42}a_{11}}{2a_{21}^2} + \frac{a_{41}}{2a_{21}}\right)\ln\left|\phi\left(\bar{z}_m^*\right)\right| + f\left(\bar{z}_m^*\right), \tag{4.68}$$

where $\bar{z}_m^*$ is given by Eq. (4.53).

The solution of the problem (4.67), (4.68) of the drying at Stage 2 has the form:

$$\bar{z}_m = \frac{B_1}{\Gamma_{01}} \pm \sqrt{\left(\frac{B_1}{\Gamma_{01}}\right)^2 + \frac{2}{\Gamma_{01}}\left[-B_1\bar{z}_m^* + \Gamma_{01}\frac{\bar{z}_m^{*2}}{2} + \frac{1}{L_0\rho_L}\Omega_1\left(t - t^*\right)\right]},$$

and of the problem (4.68), (4.69):

$$\bar{z}_{m1}=\frac{B_2}{\Gamma_{02}}\pm\sqrt{\left(\frac{B_2}{\Gamma_{02}}\right)^2+\frac{2}{\Gamma_{02}}\left[\frac{1}{L_0\gamma_L}\Omega_2\left(t-t^*\right)\right]}.$$

The relative moisture content at Stage 2 of drying $(t>t^*)$ is determined by the expression:

$$\alpha_m=\frac{B_1}{\Gamma_{01}}-\sqrt{\left(\frac{B_1}{\Gamma_{01}}\right)^2+\frac{2}{\Gamma_{01}}\left[-B_1\tilde{\bar{z}}_m^*+\Gamma_{01}\frac{\tilde{\bar{z}}_m^{*2}}{2}+\frac{1}{L_0\rho_L}\Omega_1\left(t-t^*\right)\right]}-$$
$$-\frac{B_2}{\Gamma_{02}}+\sqrt{\left(\frac{B_2}{\Gamma_{02}}\right)^2+\frac{2}{\Gamma_{02}}\left[\frac{1}{L_0\rho_L}\Omega_2\left(t-t^*\right)\right]}.$$

Let's proceed to the quantitative analysis of the obtained correlations.

Based on the obtained formulas, a quantitative analysis is conducted. The study examines the variation of relative moisture content α_m over time for different temperatures and external electric field intensities. Results are presented in **Fig. 4.6–4.7**.

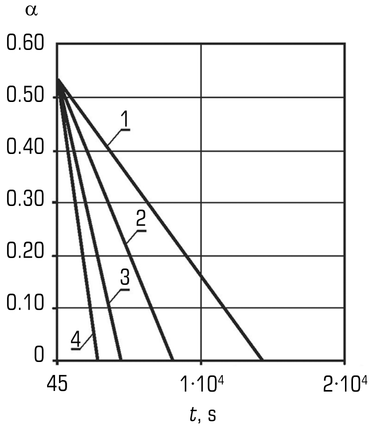

Fig. 4.6 Temporal dependence of the relative moisture content of the layer during the second stage of drying at $E=200$ V/m for temperatures of 300 K, 310 K, 320 K, and 330 K

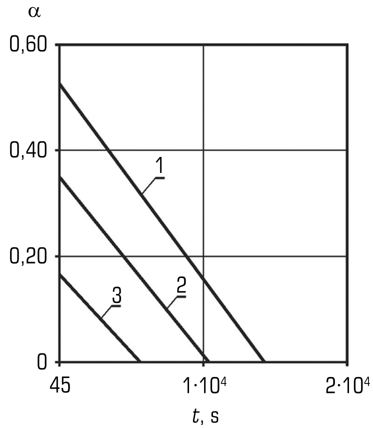

Fig. 4.7 Temporal dependence of the relative moisture content of the layer during the second stage of drying for a temperature of 300 K at $E = 200$ V/m, 400 V/m, and 1000 V/m

Fig. 4.6 and **4.7** illustrate the nature of the temporal dependence of relative moisture content for different temperatures (**Fig. 4.6**) and different intensities of the external electric field applied during the first stage of drying (**Fig. 4.7**). It follows that this dependence is linear. The drying rate (slope of the curve) during the second stage is determined by the temperature. The initial humidity level in the second stage of drying is lower for higher field intensities applied during the first stage.

4.3.6 ESTIMATION OF TEMPERATURE CHANGE IN THE LAYER DUE TO THE INFLUENCE OF THE ELECTRIC FIELD

In this work, the change in temperature due to Joule heating, caused by the action of the electric field in the first stage of drying, is neglected. Let's substantiate this by estimating such a change for the maximum electric field intensity ($E = 1000$ V/m).

The heat generation density in the liquid according to Joule-Lenz's law is given by:

$$Q = \sigma E^2 t,$$

where σ is the electrical conductivity coefficient. This heat is used to heat the liquid and the skeleton. It is possible to assume that the heating time is significantly greater than the heat transfer time from the liquid to the skeleton, meaning that the heating of the layer is considered uniform.

The thermal balance equation is:

$$\Pi\sigma E^2 t = \left[\rho_s C_s (1-\Pi) + \rho_L C_L \Pi\right]\Delta T,$$

where C_s and C_L are the specific heat capacities of the dry material and liquid, respectively. From this equation, let's obtain:

$$\Delta T = \frac{\Pi\sigma E^2 t}{\rho_s C_s (1-\Pi) + \rho_L C_L \Pi}.$$

Let E = 1000 V/m, the density of dry pine wood $\rho_s = 500 \text{kg/m}^3$, water $\rho_L = 1000 \text{kg/m}^3$, porosity $\Pi = 0.291$, specific heat capacities C_s = 1.604 kJ/(kg·K), C_L = 4.19 kJ/(kg·K), and σ = 10^{-3} S/m [37].

A quantitative estimate for the rate of temperature change gives:

$$\frac{\Delta T}{t} \approx 10^{-4} \text{K/s}.$$

For the above-mentioned durations of the first stage of drying, this results in a temperature change of fractions of a degree, which can be neglected.

4.4 THE INFLUENCE OF ELECTROOSMOSIS ON BILATERAL CONVECTIVE DRYING OF A POROUS LAYER

Let's consider the formulation and solution of the problem of drying a porous layer that is in contact with an environment consisting of a mixture of air and vapor, under the influence of convective airflow and the enhancement of this process by an external electric field.

The objective here is to formulate and solve the problem of drying an initially moisture-saturated porous layer, stimulated by convection and electroosmosis. As in previous sections, the quasi-homogeneous approximation is used, based on the application of macroscopic equations analogous to those in an individual pore, but with effective transport coefficients, while neglecting film transport.

4.4.1 OBJECT OF STUDY AND PROBLEM FORMULATION

Let's consider an initially moisture-saturated porous layer, referenced to a Cartesian coordinate system (x, y, z), occupying the region $0 < z < L_0$. Let's investigate the effect of electroosmosis on the drying process of the porous layer under convective mass exchange at one of the surfaces (Surface 1). The temperature of the air and the layer is assumed to be equal. Since the vapor at the pore surface is saturated, while the surrounding medium is unsaturated, vapor flows outward. As a result, a zone of dried pores filled with a mixture of air and vapor forms in the material, with air and vapor considered as separate components of the gas phase. During the drying process, this zone expands deeper into the material. The coordinate of the moving boundary is denoted as $z = L_m$.

To intensify the drying process by electroosmotic moisture removal from the porous layer, a constant potential difference is applied between Surfaces 1 and 2. Due to the action of the field on the electric charge of the diffuse part of the double electric layer near the solid-liquid interface, an additional (ponderomotive) force arises, inducing an electroosmotic moisture flow j_3 toward Surface 2. In opposition to the osmotic pressure, capillary forces arise, leading to a filtration flow j_2.

On Surface 2, moisture removal occurs via convective evaporation of the saturated vapor. Due to the displacement of the moving boundary and neglecting film transport, the vapor at the opposite side (Surface 2) of the porous layer remains saturated. The vapor flux from Surface 2 is given by [1, 38, 39]:

$$j_4 = \beta_2 \left(\rho_n - \rho_0 \right) \text{ at } z = 0. \tag{4.69}$$

As a result of the combined effects of the forces that arise during drying, the relative moisture content in the porous layer changes. Using the notations adopted in Section 2, the transport of dry air and vapor in the dried region $L_0 < z < L_m$ under a quasi-stationary process, while neglecting the flow of dry air into the pores, is described by the nonlinear Stefan-Maxwell differential equation (4.43) [31].

The convective mass transfer conditions at the surface $z = L_0$ are:

$$\rho_v \frac{K}{\mu_g} \frac{\partial P}{\partial z} + D \frac{\partial \rho_v}{\partial z} = -j,\ \rho_a = \rho_{a0}, \tag{4.70}$$

where $j = \beta\left(\rho_{v1} - \rho_0\right)$.

The phase transition from liquid to vapor at the gas-liquid interface $z = L_m$ is accounted for by prescribing the density of the saturated vapor at this surface, which depends on temperature and is determined by equation (4.20). At the phase transition surface $z = L_m$:

$$< \rho_v = \rho_n, \tag{4.71}$$

where ρ_n is the density of the saturated vapor.

4.4.2 SOLUTION AND QUANTITATIVE ANALYSIS OF THE PROBLEM

From the solution of the problem about convective-diffusive vapor transport [2], the vapor density η_1 at the wall $k=1$ is determined as follows:

$$\eta_1 = -\left(A + B\bar{z}_m^*\right) + \sqrt{U + S\bar{z}_m^* + B^2\bar{z}_m^{*2}}, \tag{4.72}$$

where

$$A = \frac{(1+a)}{b}, \quad B = -\beta' A, \quad U = (A+1)^2, \quad S = 2B(A+\eta_0), \quad \eta_0 = \frac{\rho_0}{\rho_n},$$

$$a = \frac{D'M_a}{\left(\dfrac{K_g}{\mu_g}\right)\rho_{a0}RT}, \quad b = \frac{\rho_n}{\rho_{a0}}\frac{M_a}{M_v}, \quad \beta' = \frac{L_0\beta}{D'}, \quad \bar{z}_m^* = 1 - \bar{z}_m, \tag{4.73}$$

$$\rho_a = \rho_{a1}\xi, \quad \rho_v = \rho_n\eta, \quad z = L_0\bar{z}, \quad \eta_1 = \eta\big|_{\bar{z}=1}.$$

The convective-diffusive flux j_1:

$$j = H\left[-\left(a_1 + B\bar{z}_m^*\right) + \sqrt{U + S\bar{z}_m^* + B^2\bar{z}_m^{*2}}\right], \quad a_1 = A + \eta_0. \tag{4.74}$$

Since the moisture reserve in the porous layer is limited, drying occurs in two stages. In the first stage, a filtration-osmotic regime is established, which lasts until the electroosmotic and filtration fluxes equalize. The capillary pressure forces induce the flow j_2 equation (4.22):

$$j_2 = \Pi\rho_L\upsilon_L = \rho_L\frac{K_L}{\mu_L}\frac{P_K}{L_0\left(1-\bar{z}_m^*\right)}\Pi. \tag{4.75}$$

To determine the electroosmotic flow, let's use the quasi-homogeneous approximation for the porous body. The electroosmotic liquid flow in the porous layer is given by equation (4.25):

$$j_3 = \gamma_L v_{osm}\Pi = \frac{\gamma_L K_L \Pi}{\mu_L}\frac{2\bar{\eta}\varepsilon_\rho E}{\bar{R}\left[\left(1-\kappa_m\right)+\varepsilon_\rho\kappa_m\right]}. \tag{4.76}$$

The critical relative moisture content at which the liquid flows balance and the second drying regime begins is determined from equation (4.27). Since the rate of liquid mass change in the drying process is defined by the vapor and liquid fluxes from the layer, let's arrive at the following Cauchy problem:

$$\frac{dz_m}{dt} = H\left[-\left(a_1 + Bz_m^*\right) + \sqrt{U + Sz_m^* + B^2 z_m^{*2}} + \frac{\tilde{K}}{1 - z_m^*} + \frac{\tilde{K}_1}{K_2\left(1 - z_m^*\right) + K_3 z_m^*}\right], \tag{4.77}$$

under the initial condition:

$$z_m^*\left(0\right) = 0, \tag{4.78}$$

where

$$\tilde{K} = \frac{\rho_L K_L P_k}{\mu_L L_0 \beta \rho_n}\Pi, \quad \tilde{K}_1 = \frac{2K_L \rho_L \Pi \varepsilon_\rho \bar{\eta} E}{\beta \rho_n \mu_L \bar{R}}, \quad K_2 = \varepsilon_\rho, \quad K_3 = 1, \quad \bar{\eta} = ZF\psi_1\sqrt{2\varepsilon\frac{C}{RT}}, \quad \varepsilon = \varepsilon_0 \varepsilon_r.$$

By substituting variables $\sqrt{U + Sz_m^* + B^2 z_m^{*2}} = \chi + z_m^* B$, Eq. (4.77) transforms into:

$$-\frac{2\left(B\chi^2 - S\chi + BU\right)}{\left(S - 2B\chi\right)^2}\frac{d\chi}{dt} = H\frac{\left(\chi - a_1\right)\left(\tilde{a}\chi^4 + \tilde{b}\chi^3 + c\chi^2 + \tilde{d}\chi + \tilde{e}\right)}{\left(\chi^2 + 2\chi B - \omega_1\right)\left(\Omega_2\chi^2 + \Omega_1\chi + \Omega_0\right)}, \tag{4.79}$$

where

$$\omega_1 = S + U, \quad \Omega_2 = K_2 - K_3, \quad \Omega_1 = 2K_2 B, \quad \Omega_0 = -K_2\omega_1 + K_3 U, \quad \tilde{a} = 1, \quad \tilde{b} = \frac{\Omega_1 + 2B\Omega_2}{\Omega_2},$$

$$\tilde{c} = \frac{\Omega_0 + 2B\Omega_1 - \Omega_2\omega_1 + 2\tilde{K}B\Omega_2 + 2\tilde{K}_1 B}{\Omega_2}, \quad \tilde{e} = \frac{2\tilde{K}B\Omega_0 - \Omega_0\omega_1 - 2\tilde{K}_1 B\omega_1}{\Omega_2},$$

$$\tilde{d} = \frac{2B\Omega_0 - \Omega_1\omega_1 + 2\tilde{K}B\Omega_1 + 4\tilde{K}_1 B^2}{\Omega_2}. \tag{4.80}$$

Equation (4.79) is written in the form:

$$-\frac{2\left(B\chi^2 - S\chi + BU\right)\left(\chi^2 + 2\chi B - \omega_1\right)\left(\Omega_2\chi^2 + \Omega_1\chi + \Omega_0\right)}{\left(S - 2B\chi\right)^2\left(\chi - a_1\right)\left(\chi - c_1\right)\left(\chi - c_2\right)\left(\chi - c_3\right)\left(\chi - c_4\right)}\frac{d\chi}{dt} = H\Omega_2, \tag{4.81}$$

where $c_i=\chi_i,\ i=\overline{1,4}$ are roots of Eq. $\left(\tilde{a}\chi^4+\tilde{b}\chi^3+c\chi^2+\tilde{d}\chi+\tilde{e}\right)=0$. The solution of Eq. (4.81) has the form:

$$D_1\ln\left|\frac{S-2B\chi}{S-2B\sqrt{U}}\right|+D_2\left[\frac{1}{S-2B\chi}-\frac{1}{S-2B\sqrt{U}}\right]+D_3\left[\frac{1}{\left(S-2B\chi\right)^2}-\frac{1}{\left(S-2B\sqrt{U}\right)^2}\right]+$$

$$+R_3\ln\left|\frac{\chi-c_1}{\sqrt{U}-c_1}\right|+R_4\ln\left|\frac{\chi-c_2}{\sqrt{U}-c_2}\right|+R_5\ln\left|\frac{\chi-c_3}{\sqrt{U}-c_3}\right|+R_6\ln\left|\frac{\chi-c_4}{\sqrt{U}-c_4}\right|=H\Omega_2 t, \qquad (4.82)$$

where $D_1=-\frac{R_2}{8B^3},\ D_2=-\frac{1}{4B^2}\left(\frac{R_2S}{B}+R_1\right),\ D_3=\frac{1}{4B}\left(\frac{R_2S^2}{4B^2}+\frac{R_1S}{2B}+R_0\right),\ R_0,R_1\ldots R_6$ are solutions of the following system of algebraic equations:

$$\sum_{i=0}^{2}d_{i,6-j}R_i+\sum_{i=3}^{6}b_{i-2,6-j}R_i=4B\Omega_{1,6-j}\ \left(j=\overline{0,6}\right), \qquad (4.83)$$

$$d_{0,6}=d_{16}=d_{05}=0,\ \ d_{2,6}=d_{1,5}=d_{0,4}=1,\ \ d_{2,5}=d_{1,4}=d_{0,3}=\tilde{b},$$
$$d_{2,4}=d_{1,3}=d_{0,2}=\tilde{c},\ \ d_{2,3}=d_{1,2}=d_{0,1}=\tilde{d},\ \ d_{2,2}=d_{1,1}=d_{0,0}=\tilde{e},$$

$$b_{i,6}=8B^3a_{i+2,3},\ \ b_{i,5}=8Ba_{i+2,2}+12B^2Sa_{i+2,3},\ \ b_{i,4}=8B^3a_{i+2,1}+12B^2Sa_{i+2,2}-6BS^2a_{i+2,3},$$
$$b_{i,3}=8B^3a_{i+2,0}+12B^2Sa_{i+2,1}-6BS^2a_{i+2,2}+S^3a_{4,3},\ \ b_{i,2}=12B^2Sa_{i+2,0}-6BS^2a_{i+2,1}+S^3a_{4,2},$$
$$b_{i,1}=-6BS^2a_{i+2,0}+S^3a_{4,1},\ \ b_{i,1}=S^3a_{4,0},$$

$$a_{i+2,1}=1,\ \ a_{3,2}=-\left(c_4+c_2+c_3\right),\ \ a_{3,1}=\left(c_2+c_3\right)c_4+c_2c_3,\ \ a_{3,0}=-c_2c_3c_4,$$
$$a_{4,2}=-\left(c_4+c_1+c_3\right),\ \ a_{4,1}=\left(c_1+c_3\right)c_4+c_1c_3,\ \ a_{4,0}=-c_1c_3c_4,$$
$$a_{5,2}=-\left(c_2+c_1+c_4\right),\ \ a_{5,1}=\left(c_1+c_2\right)c_4+c_1c_2,\ \ a_{5,0}=-c_1c_4c_2,$$
$$a_{6,2}=-\left(c_2+c_1+c_3\right),\ \ a_{6,1}=\left(c_1+c_2\right)c_3+c_1c_2,\ \ a_{6,0}=-c_1c_3c_2,$$
$$a_{0,4}=B,\ \ a_{0,3}=2B^2-S,\ \ a_{0,2}=\omega_1B-2BS+BU,\ \ a_{0,1}=\omega_1S+2B^2U,\ \ a_{0,0}=-BU\omega_1,$$

$$\Omega_{16}=a_{0,4}\Omega_2,\ \ \Omega_{15}=a_{0,4}\Omega_1+a_{0,3}\Omega_2,\ \ \Omega_{14}=a_{0,4}\Omega_0+a_{0,3}\Omega_1+a_{0,2}\Omega_2,$$
$$\Omega_{13}=a_{0,3}\Omega_0+a_{0,2}\Omega_1+a_{0,1}\Omega_2,\ \ \Omega_{12}=a_{0,2}\Omega_0+a_{0,1}\Omega_1+a_{0,0}\Omega_2,$$
$$\Omega_{11}=a_{0,1}\Omega_0+a_{0,0}\Omega_1,\ \ \Omega_{10}=a_{0,0}\Omega_0.$$

The transcendental equation (4.83) establishes the relationship between the relative moisture content in the porous layer and time in the first drying regime. When the relative moisture content reaches the value $\bar{z}_m = \bar{z}_{kr}$, the evaporation regime begins, where the change in relative moisture content is determined by the following Cauchy problem:

$$\frac{d\bar{z}_m^*}{dt} = H\left[-\left(a_1 + B\bar{z}_m^*\right) + \sqrt{U + S\bar{z}_m^* + B^2\bar{z}_m^{*2}} - \frac{\beta_2}{\beta}\left(1 - \eta_{02}\right)\right], \qquad (4.84)$$

under the condition that at $t = t_{kr}$, $\bar{z}_m^* = 1 - \bar{z}_{kr}$.

By introducing $a_2 = a_1 + \left(1 - \eta_{02}\right)\beta_2 / \beta$, let's obtain the equation:

$$\frac{d\bar{z}_m^*}{dt} = H\left[-\left(a_2 + B\bar{z}_m^*\right) + \sqrt{U + S\bar{z}_m^* + B^2\bar{z}_m^{*2}}\right], \qquad (4.18)$$

which, upon introducing the variable χ, transforms into:

$$\frac{2\left(\chi S - BU - B\chi^2\right)}{\left(2B\chi - S\right)^2\left(\chi - a_2\right)}\frac{d\chi}{dt} = H, \qquad (4.85)$$

under the initial condition:

$$t = t_{kr} \;\; \chi = \chi_{kr}, \qquad (4.86)$$

where

$$\chi_{kr} = \sqrt{U + S\bar{z}_{kr}^* + B^2\bar{z}_{kr}^{*2}} - \bar{z}_{kr}^* B, \quad \bar{z}_{kr}^* = 1 - \bar{z}_{kr}^*,$$

and t_{kr} is determined from the solution of the Cauchy problem (4.75), (4.76).

Integration of equation (4.85) under condition (4.86) leads to the following transcendental equation for χ:

$$\frac{C_1}{4B^2}\ln\frac{\left|2B\chi - S\right|}{\left|2B\chi_{kr} - S\right|} - \frac{1}{2B}\left(\frac{C_1 S}{4B^2} + C_2\right)\left[\frac{1}{S - 2B\chi} - \frac{1}{S - 2B\chi_{kr}}\right] +$$

$$+ C_3\ln\left|\frac{\chi - a_2}{\chi_{kr} - a_2}\right| = H\left(t - t_{kr}\right), \qquad (4.87)$$

where

$$C_1 = \frac{2B\left(-S^2 + 4B^2U\right)}{\left(S - 2a_2B\right)^2}, \quad C_2 = \frac{2\left(Ba_2 - S\right)\left(-S^2 + 4B^2U\right)}{\left(S - 2a_2B\right)^2}, \quad C_3 = \frac{-2BU - 2Ba_2^2 + 2Sa_2}{\left(S - 2a_2B\right)^2}.$$

Equation (4.87) establishes the relationship between relative moisture content and time over the range $\bar{z}_{kr} - 0$. Graphs of the dependence of the layer's relative moisture content on the mass transfer coefficient, electric field intensity, and temperature are presented in **Fig. 4.8–4.11**. Calculations were performed for a coarse-porous material, where *D'* represents the molecular diffusion of the vapor-air mixture, which is a function of temperature.

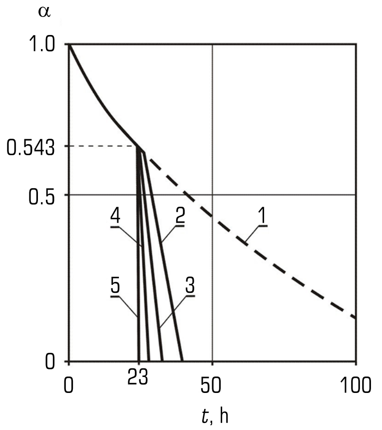

Fig. 4.8 Dependence of relative saturation on the mass transfer coefficient β_2

In **Fig. 4.8**, the mass transfer coefficients β_2 = 0.01; 0.05; 0.1; 0.5; 1 (curves 1–5, respectively), with *E* = 200 V/m (β = 0.1; *T* = 300 K, $L_0 = 0.1$ m, $\bar{z}_{kr} = 0.543$, $t_{kr} = 23$ h), correspond to complete dehydration times of 139; 39.751; 31.305; 23.733; and 23.244 hours, respectively.

In **Fig. 4.9**, curves 1 and 2 correspond to the electric field intensities of *E* = 200 V/m and *E* = 400 V/m. Here, $L_0 = 0.5$ m, *T* = 300 K, and β = 0.1. The points where curve branching occurs correspond to the critical values of $\bar{z}_m = \bar{z}_{kr}$ for humidity. The curve branches after the branching point, from right to left, correspond to mass transfer coefficient values of β_2 = 0.01; 0.05; 0.1; 0.5; and 1.

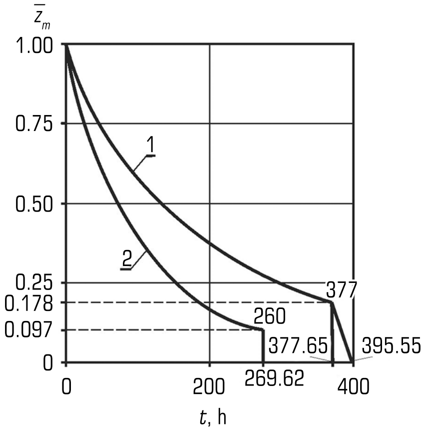

Fig. 4.9 The effect of electric field intensity on humidity variation over time

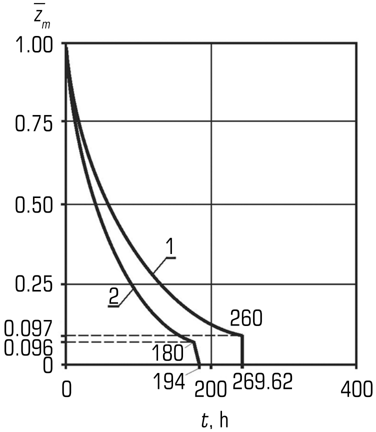

Fig. 4.10 Time dependence of relative moisture content for different temperatures

Thus, at $E = 200$ V/m, $\bar{z}_{kr} = 0.178$, $t_{kr} = 377$ hours, the total dehydration time for $\beta_2 = 0.01$ is 395.552 hours, and for $\beta_2 = 1$ it is 377.65 hours.

For $E = 400$ V/m, $\kappa_{kr} = 0.097$, $t_{kr} = 260$ hours, the total dehydration time for $\beta_2 = 0.01$; 0.05; 0.1; 0.5; 1 is 269.62; 261.11; 260.555; 260.185; 260.185 hours, respectively.

Quantitative calculations, the graphical results of which are shown in **Fig. 4.10**, were conducted for $E = 400$ V/m, $\beta = 0.1$; $L_0 = 0.5$ m. At $\bar{z}_{kr} = 0.097$, $t_{kr} = 260$ hours, and temperature $T = 300$ K, the corresponding total dehydration times for mass transfer coefficient values of $\beta_2 = 0.01$; 0.05; 0.1; 0.5; 1 are 269.62; 261.11; 260.555; 260.185; 260.185 hours.

For $\bar{z}_{kr} = 0.096$, $t_{kr} = 180$ hours, and temperature $T = 310$ K, the total dehydration times for the same β_2 values are 185.74; 180.82; 180.205; 180; 180 hours, respectively.

CONCLUSIONS

Based on the electroosmotic drying model, a series of problems have been solved regarding the influence of external constant electric field parameters on moisture mass transfer in pores. The effects of the following parameters have been investigated:

a) boundary layer properties;

b) electric field intensity in unilateral natural drying;

c) moisture exchange coefficients in convective drying when the second side is saturated with moisture (a process relevant to basement flooding);

d) bilateral drying.

It has been demonstrated that in bilateral drying the electric field affects the process primarily during the first stage of drying, when the ponderomotive force dominates over the capillary force. As a result, the relative moisture content curve exhibits a breakpoint, both in natural and convective drying. It has been shown that the temperature change induced by a constant electric field in a moist body can be neglected. Increasing the intensity of the electric field enhances the drying process. Numerical results are provided for cement stone material.

REFERENCES

1. Burak, Ya., Chaplia, Ye., Nahirnyi, T. et al. (2004). Fizyko-matematychne modeliuvannia skladnykh system. Lviv: SPOLOM, 264.
2. Haivas, B. I. (2004). Pro vplyv elektroosmosu na dvostoronnie konvektyvne osushennia porystoho sharu. Volynskyi matematychnyi visnyk. Seriia prykladna matematyka, 2 (11), 74–85.
3. Chaplya, Ye., Hayvas, B., Torskyy, A. (2015). Construction of the solution of the thermal-convective drying problem for porous solids in drying plants. Mathematical Modeling and Computing, 2 (1), 1–15. https://doi.org/10.23939/mmc2015.01.001
4. Sokolovskyy, Y., Drozd, K., Samotii, T., Boretska, I. (2024). Fractional-Order Modeling of Heat and Moisture Transfer in Anisotropic Materials Using a Physics-Informed Neural Network. Materials, 17 (19), 4753. https://doi.org/10.3390/ma17194753

5. Hachkevych, O., Musii, R., Melnyk, N. (2023). Problems of Thermomechanics of Multilayered Electroconductive Bodies Under the Action of the Pulsed Electromagnetic Fields with Modulation of Amplitude. Advances in Mechanics, 185–206. https://doi.org/10.1007/978-3-031-37313-8_11
6. Zhuravchak, L. M. (2007). Matematychne modeliuvannia protsesiv poshyrennia teplovoho ta elektromahnitnoho poliv u neodnoridnykh seredovyshchakh metodamy pryhranychnykh elementiv ta skinchennykh riznyts. [Extended abstract of doctors thesis].
7. Dukhin, S. S. (1975). Elektroprovodnost y elektrokynetycheskye svoistva dyspersnikh system. Kyiv: Naukova dumka, 246.
8. Decker, Ž., Tretjakovas, J., Drozd, K., Rudzinskas, V., Walczak, M., Kilikevičius, A. et al. (2023). Material's Strength Analysis of the Coupling Node of Axle of the Truck Trailer. Materials, 16(9), 3399. https://doi.org/10.3390/ma16093399
9. Tokarchuk, M. V. (2024). Kinetic coefficients of ion transport in a porous medium based on the Enskog – Landau kinetic equation. Mathematical Modeling and Computing, 11 (4), 1013–1024. https://doi.org/10.23939/mmc2024.04.1013
10. Sokolovskyy, Ya. I., Boretska, I. B., Gayvas, B. I., Kroshnyy, I. M., Nechepurenko, A. V. (2021). Mathematical modeling of convection drying process of wood taking into account the boundary of phase transitions. Mathematical Modeling and Computing, 8 (4), 830–841. https://doi.org/10.23939/mmc2021.04.830
11. Borovytskyi, M. Y., Lysenko, L. L., Rynda, O. F., Mishchuk, N. O. (2014). Rehuliuvannia vlastyvostei dyspersii dlia yikh elektrokinetychnoi obrobky. Naukovi visti NTUU "KPI", (3), 100–106.
12. Barinova, N. O. (2016). Neliniini elektroforez ta elektroosmos dlia odynychnykh chastynok ta skladnykh system. [Extended abstract of Candidate's thesis; Institute of Colloid Chemistry and Water Chemistry, NAS of Ukraine].
13. Malyarenko, V. V., Makarov, A. S. (2000). Elektropoverkhnostnye svoystva vspenennykh kontsentrirovannykh suspenziy kremnezema i uglya. Ukrainskyi khimichnyi zhurnal, 66 (9-10), 84–87.
14. Myshchuk, N. A., Lysenko, L. L., Kornilovych, B. Y., Barinova, N. O. (2002). Teoreticheskiy analiz zakonomernostey elektroosmoticheskogo transporta zhidkosti cherez diafragmu. Khimia i tekhnologiya vody, 24 (4), 328–351.
15. Berezniak, O. O. (1999). Zastosuvannia yavyshcha elektroosmosu pry znevodnenni kaolinu. Zbahachennia korys. kopalyn, 4 (45), 100–104.
16. Lysenko, L. L. (2002). Intensyfikatsiia masoperenosu pry elektrokinetychnii ochystsi hruntu. [Extended abstract of Candidate's thesis; Institute of Colloid Chemistry and Water Chemistry, NAS of Ukraine].
17. Shevchenko, R. O. (2012). Upravlinnia elektrokinetychnymy protsesamy dlia poperedzhennia i podolannia avarii pry burinni sverdlovyn na naftu ta haz [Extended abstract of Candidate's thesis; National Technical University "Kharkiv Polytechnic Institute"].
18. Pushkarov, O., Zubko, O., Sevruk, I., Dolin, V. (2022). Use of mineral proton-conductive membranes for electroosmotic fractionation of the hydrogen isotopes. Geochemistry of Technogenesis, 35, 65–68. https://doi.org/10.32782/geotech2022.35.12

19. Musii, R., Melnyk, N., Dmytruk, V. (2024). Thermal stresses in bimetallic plate under induction heating by nonstationary electromagnetic field. Journal of Thermal Stresses, 47 (11), 1539–1551. https://doi.org/10.1080/01495739.2024.2415030
20. Musii, R., Dmytruk, V., Oryshchyn, O., Kushka, B., Shayner, H., Huk, L. (2024). Analysis of Thermal Modes of a Bimetallic Tube Under Short-Term Induction Heating. 2024 IEEE 19th International Conference on the Perspective Technologies and Methods in MEMS Design (MEMSTECH), 16–19. https://doi.org/10.1109/memstech63437.2024.10620050
21. Musii, R., Dmytruk, V., Voloshyn, M. M., Kushka, B., Nakonechny, R., Huk, L. (2023). Computer Analysis of Nonstationary Thermoelastic Processes in an Electrically Conductive Plate during Pulse Electromagnetic Treatment. 2023 IEEE XXVIII International Seminar/Workshop on Direct and Inverse Problems of Electromagnetic and Acoustic Wave Theory (DIPED), 221–224. https://doi.org/10.1109/diped59408.2023.10269468
22. Gayvas, B., Burak, Y., Kondrat, V. (2005). Do matematychnoho modeliuvannia ta vyvchennia protsesu osushennia porystykh til. Fiz.-mat. modeliuvannia ta inform. tekhnolohii, 1, 20–29.
23. Gayvas, B. I., Markovych, B. M., Dmytruk, A. A., Havran, M. V., Dmytruk, V. A. (2023). Numerical modeling of heat and mass transfer processes in a capillary-porous body during contact drying. Mathematical Modeling and Computing, 10(2), 387–399. https://doi.org/10.23939/mmc2023.02.387
24. Severyn, O. A. (2008). Rozrobka protsesu ta aparaturnoho osnashchennia kombinovanoho heliosushinnia plodovoi syrovyny z avtonomnym enerhopostachanniam. [Extended abstract of Candidate's thesis; Kharkiv State University of Food and Trade].
25. Fariseev, A. G. (2014). Rozrobka aparata dlia zharenia miasa v umovakh elektroosmosu. [Extended abstract of Candidate's thesis; Kharkiv State University of Food and Trade].
26. Drachov, V. I. (2000). Tekhnolohiia zbahachennia ta kompleksnoho vykorystannia vidkhodiv staleplavylnoho vyrobnytstva. [Extended abstract of Candidate's thesis; Kryvyi Rih Technical University].
27. Kostyuk, G. Ya., Kostyuk, O. G., Burkov, M. V, Golubovsky, I. A., Bulko, M. P., Bandura, L. O. et al. (2020). Pancreatic secretion and pressure biomechanics in pancreatic acinus. Clinical Anatomy and Operative Surgery, 19 (1), 6–12. https://doi.org/10.24061/1727-0847.19.1.2020.1
28. Kheifitc, L. I., Neimark, A. V. (1982). Mnogofaznye protcessy v poristykh sredakh. Moscow: Khimiia, 320.
29. Gayvas, B. I., Dmytruk, V. A. (2022). Investigation of drying the porous wood of a cylindrical shape. Mathematical Modeling and Computing, 9 (2), 399–415. https://doi.org/10.23939/mmc2022.02.399
30. Burak, Ya., Kondrat, V., Haivas, B. (2002). Do matematychnoho modeliuvannia protsesiv sushky porystykh til. Informatychno-matematychne modeliuvannia skladnykh system – MIMUZ2002. Lviv: TsMM IPPMM im. Ya. S. Pidstryhacha NAN Ukrainy, Vyd-vo Akhil, 153–159.
31. Gayvas, B. I., Dmytruk, V. A., Semerak, M. M., Rymar, T. I. (2021). Solving Stefan's linear problem for drying cylindrical timber under quasi-averaged formulation. Mathematical Modeling and Computing, 8 (2), 150–156. https://doi.org/10.23939/mmc2021.02.150

32. Kondrat, V. F., Kubik, Yu., Chaplia, Ye. Ya. (2000). Vzaiemodiia mekhanotermoelektrodyfuziinykh protsesiv v porystomu nasychenomu seredovyshchi. Mashynoznavstvo, 8, 3–9.
33. Gayvas, B., Dmytruk, V., Kaminska, O., Pastyrska, I., Dmytruk, A., Nezgoda, S. (2020). Simulation of Crack Resistance of Mustard in Pulsed Drying Mode. 2020 IEEE 15th International Conference on Computer Sciences and Information Technologies (CSIT), 91–94. https://doi.org/10.1109/csit49958.2020.9321941
34. Gayvas, B., Markovych, B., Dmytruk, A., Dmytruk, V., Kushka, B., Senkovych, O. (2023). Study of Contact Drying Granular Materials in Fluidized Bed Dryers. 2023 IEEE XXVIII International Seminar/Workshop on Direct and Inverse Problems of Electromagnetic and Acoustic Wave Theory (DIPED). Tbilisi, 238–241. https://doi.org/10.1109/diped59408.2023.10269464
35. Gayvas, B. I. (2004). On the influence of electroosmosis on two-sided convective drying of a porous layer. Volyn Mathematical Bulletin, 2 (11), 74–85.
36. Gayvas, B., Markovych, B., Dmytruk, A., Havran, M., Dmytruk, V. (2024). The methods of optimization and regulation of the convective drying process of materials in drying installations. Mathematical Modeling and Computing, 11 (2), 546–554. https://doi.org/10.23939/mmc2024.02.546
37. Polos, A. V. (2006). Pidvyschennia efektyvnosti konvektyvnoho sushinnia pylomaterialiv (na prykladi umovnoho material). [Dissertation].
38. Dmytruk, A. (2024). Modeling mass transfer processes in multicomponent capillary-porous bodies under mixed boundary conditions. Mathematical Modeling and Computing, 11 (4), 978–986. https://doi.org/10.23939/mmc2024.04.978
39. Gayvas, B. I. (2003). Dynamika vologosti porystogo sharu pry osushuvanni z odniyeyi poverkhni. Konferentsiia profesorsko-vykladatskoho skladu DU “Lvivska politekhnika”. Lviv, 7–9.
40. Grinchik, N. N. (1991). Protcessy perenosa v poristykh sredakh, elektrolitakh i membranakh. Minsk: ITMO im. A.V. Lykova AN BSSR, 310.